

Electrochemical reduction of carbon dioxide on copper-based cathodes in  
electrochemical tubular fixed bed reactor



A Thesis Submitted in Partial Fulfillment of the Requirements  
for the Degree of Master of Engineering in Chemical Engineering

Department of Chemical Engineering

FACULTY OF ENGINEERING

Chulalongkorn University

Academic Year 2021

Copyright of Chulalongkorn University

ปฏิกิริยารีดักชันเชิงเคมีไฟฟ้าของก๊าซคาร์บอนไดออกไซด์บนขั้วแคโทดทองแดงในเครื่องปฏิกรณ์  
เคมีไฟฟ้าเบตนิ่งแบบท่อ



วิทยานิพนธ์นี้เป็นส่วนหนึ่งของการศึกษาตามหลักสูตรปริญญาวิทยาศาสตรมหาบัณฑิต  
สาขาวิชาวิศวกรรมเคมี ภาควิชาวิศวกรรมเคมี  
คณะวิศวกรรมศาสตร์ จุฬาลงกรณ์มหาวิทยาลัย  
ปีการศึกษา 2564  
ลิขสิทธิ์ของจุฬาลงกรณ์มหาวิทยาลัย

Thesis Title                      Electrochemical reduction of carbon dioxide on copper-based cathodes in electrochemical tubular fixed bed reactor

By                                      Miss Kanjira Janya

Field of Study                      Chemical Engineering

Thesis Advisor                      Associate Professor Palang Bumroongsakulsawat, Ph.D.

---

Accepted by the FACULTY OF ENGINEERING, Chulalongkorn University in  
Partial Fulfillment of the Requirement for the Master of Engineering

----- Dean of the FACULTY OF  
ENGINEERING  
(Professor SUPOT TEACHAVORASINSKUN, D.Eng.)

THESIS COMMITTEE

----- Chairman  
(Associate Professor SUPHOT PHATANASRI, D.Eng.)

----- Thesis Advisor  
(Associate Professor Palang Bumroongsakulsawat, Ph.D.)

----- Examiner  
(Assistant Professor Rungthiwa Methaapanon, Ph.D.)

----- External Examiner  
(Pongkarn Chakthranont, Ph.D.)

กัญยจิรา จรรยา : ปฏิกริยารีดักชันเชิงเคมีไฟฟ้าของก๊าซคาร์บอนไดออกไซด์บนขั้วแคโทดทองแดงในเครื่องปฏิกรณ์เคมีไฟฟ้าเบดนิ่งแบบท่อ. ( Electrochemical reduction of carbon dioxide on copper-based cathodes in electrochemical tubular fixed bed reactor) อ.ที่ปรึกษาหลัก : ผศ. ดร.พลัง บำรุงสกุลสวัสดิ์

ปฏิกริยารีดักชันเชิงเคมีไฟฟ้าของก๊าซคาร์บอนไดออกไซด์ถูกใช้ในการลดปริมาณก๊าซคาร์บอนไดออกไซด์ในชั้นบรรยากาศโดยการแลกเปลี่ยนโปรตอนและอิเล็กตรอน โดยการกระจายตัวของผลิตภัณฑ์ที่เกิดขึ้นจะขึ้นกับขั้วแคโทดซึ่งคอปเปอร์คือโลหะที่มีคุณสมบัติและความสามารถในการเร่งการเปลี่ยนก๊าซคาร์บอนไดออกไซด์เป็นสารประเภทไฮโดรคาร์บอน เช่น ก๊าซเอทิลีน ด้วยปฏิกริยารีดักชัน แต่ปัญหาหลักคือค่าการละลายของก๊าซคาร์บอนไดออกไซด์ในสารละลายอิเล็กโทรไลต์มีค่าน้อยที่อุณหภูมิห้องและความดันบรรยากาศส่งผลต่อการถ่ายโอนมวลและอัตราการเกิดปฏิกริยา ในงานวิจัยนี้ประสิทธิภาพของปฏิกริยารีดักชันจะถูกพัฒนาด้วยการเพิ่มความดัน โดยใช้คอปเปอร์โพรที่มีสารละลายไอโอดีนเมอร์เป็นขั้วแคโทดในเครื่องปฏิกรณ์แบบเบดนิ่งสำหรับปฏิกริยาแบบต่อเนื่องในการเปลี่ยนก๊าซคาร์บอนไดออกไซด์เป็นก๊าซเอทิลีน โดยสังเกตการเลือกเกิดของก๊าซเอทิลีนเมื่อเพิ่มความดันของก๊าซคาร์บอนไดออกไซด์ พบว่าประสิทธิภาพของฟาราเดย์ของก๊าซเอทิลีนที่ 10 บาร์จะสูงที่สุดและสูงกว่า 3 และ 4 เท่าที่ 5 และ 3 บาร์ตามลำดับ และประสิทธิภาพของฟาราเดย์ของก๊าซคาร์บอนมอนอกไซด์จะลดลงเนื่องจากถูกใช้ป็นสารมัธยันตร์ในการเกิดก๊าซเอทิลีน นอกจากนี้ผลกระทบของความต่างศักย์ได้ทำการศึกษา พบว่าเมื่อความต่างศักย์ของเซลล์และกระแสถูกปรับให้สูงขึ้นจะส่งผลให้ประสิทธิภาพของฟาราเดย์ของเอทิลีนและคาร์บอนมอนอกไซด์ลดลงเนื่องจากโปรตรอนที่เกิดจากน้ำจะเข้ามาดูดซับที่ผิวได้ดีกว่าสารมัธยันตร์และไปยับยั้งการเกิดปฏิกริยารีดักชันเชิงเคมีไฟฟ้าของก๊าซคาร์บอนไดออกไซด์

สาขาวิชา วิศวกรรมเคมี

ลายมือชื่อนิสิต .....

ปีการศึกษา 2564

ลายมือชื่อ อ.ที่ปรึกษาหลัก .....

# # 6370019021 : MAJOR CHEMICAL ENGINEERING

KEYWORD: Ethylene, CO<sub>2</sub>RR, Electrocatalyst, Copper, Fixed bed reactor

Kanjira Janya : Electrochemical reduction of carbon dioxide on copper-based cathodes in electrochemical tubular fixed bed reactor. Advisor: Associate Professor Palang Bumroongsakulsawat, Ph.D.

CO<sub>2</sub> electrochemical reduction reaction (CO<sub>2</sub>ERR) has been investigated with an aim to eventually become a means to decrease the concentration of CO<sub>2</sub> in the atmosphere to hydrocarbons by proton and electron transfer. The product distribution strongly depends on cathode materials. Copper is a unique metal in its ability to catalyze the electrochemical reduction of CO<sub>2</sub> to various hydrocarbons including ethylene, but the main problems are the poor solubility CO<sub>2</sub> in aqueous solutions. In this study, the performance of CO<sub>2</sub>ERR is improved by increasing pressure. The ionomer copper foam is used as a cathode in the electrochemical tubular fixed bed reactor for continuous conversion of CO<sub>2</sub> to ethylene to observe the selectivity of CO<sub>2</sub> pressure. The result show faradic efficiency (FE) of ethylene on 10 bar is 2 and 6 times higher than 5 and 3 bar, respectively and FE of CO is decreased for C-C coupling to ethylene production. Moreover, The effect of cell voltages are studied by potentialstat controlling. the results show FE of ethylene and CO are decreased because protons reduce intermediated CO on the cathode surface and lead to suppress CO<sub>2</sub> reduction while cell voltage and current are increased.

Field of Study: Chemical Engineering

Student's Signature .....

Academic Year: 2021

Advisor's Signature .....

## ACKNOWLEDGEMENTS

I am grateful to Assistant Professor Palang Bumroongsakulsawat, who helped me with my thesis and provided chances, guidance, and committed engagement at every step. His vast expertise and kind advice have motivated me throughout my stay at the university. Without him, this study would never have been completed.

I want to express my sincere gratitude to my labmates for supporting me during the difficult times. I'm grateful to P'Moss, P'Kung, and Ble for their knowledge of GC, this includes consulting, using, and repairing. I'd like to thank Fluke for your support on the day when the machine had a problem; Rung and Moss for the good meal; Chilling House people for making our vacation the most enjoyable day. I appreciate Pawin and Jay who are always by my side even under pressure. I'm thankful to Chris and Tangkwa for being my best partner in lab work.

Kanjira Janya

## TABLE OF CONTENTS

	Page
.....	iii
ABSTRACT (THAI) .....	iii
.....	iv
ABSTRACT (ENGLISH) .....	iv
ACKNOWLEDGEMENTS .....	v
TABLE OF CONTENTS .....	vi
LIST OF TABLES .....	ix
LIST OF FIGURES.....	x
CHAPTER 1 .....	1
INTRODUCTION .....	1
1.1 Background .....	1
1.2 Research objective .....	3
1.3 Scope of study.....	3
1.4 Expected benefit .....	3
CHAPTER 2 .....	4
THEORY and LITERATURE REVIEWS.....	4
2.1 Theory .....	4
2.2 Literature reviews.....	8
2.2.4 Electrolyte.....	13
CHAPTER 3 .....	15
EXPERIMENTIAL .....	15

3.1 Chemicals and Materials.....	15
3.2 Methodology .....	16
CHAPTER 4 .....	19
RESULTS and DISCUSSIONS .....	19
4.1 Characterization of Cu foam electrodes.....	19
4.2 Effects of ionomer (Sustainion XA-9) coating on Cu foam.....	20
4.3 Effect of pressure .....	23
4.4 Effect of cell voltage .....	26
4.5 Effect of type of gas .....	27
CHAPTER 5 .....	29
CONCLUSIONS and SUGGESTIONS .....	29
5.1 Conclusions.....	29
5.2 Suggestions .....	30
APPENDIX .....	31
APPENDIX A.....	32
FARADIC EFFICIENCY CALCULATION.....	32
APPENDIX B.....	36
CHARACTERIZATION of CATHODES .....	36
B.1 XRD .....	36
B.2 SEM .....	37
B.3 EDX .....	39
APPENDIX C.....	43
ELECTROCHEMICAL REDUCTION PERFORMANCE .....	43
REFERENCES.....	49



VITA .....53



จุฬาลงกรณ์มหาวิทยาลัย  
**CHULALONGKORN UNIVERSITY**

## LIST OF TABLES

	Page
Table 1 The chemical equation and the corresponding standard electrode potential (V vs. SHE)[1, 6-8]. .....	5
Table 2 Characteristics of electrodeposition techniques.[11].....	7
Table 3 Faradaic Efficiencies of Various Products from the Electroreduction of CO at a Cu Electrode in Aqueous Solutions. [16].....	14
Table 4 Data of ethylene concentration from GC. (CO <sub>2</sub> 60 ml min <sup>-1</sup> and H <sub>2</sub> O 1 ml ...	33
Table 5 Data of CO concentration from IR. (CO <sub>2</sub> 60 ml min <sup>-1</sup> and H <sub>2</sub> O 1 ml min <sup>-1</sup> ) ....	33
Table 6 Data of current from potentialstat . (CO <sub>2</sub> 60 ml min <sup>-1</sup> and H <sub>2</sub> O 1 ml.....	34
Table 7 element dispersion of fresh Cu foam. ....	39
Table 8 element dispersion of I-Cu foam. ....	39
Table 9 element dispersion of Cu-elec. ....	40
Table 10 element dispersion of Cu-ink.....	40
Table 11 element dispersion of post run Cu foam at condition 3 bar.....	41
Table 12 element dispersion of post run I-Cu foam at condition 3 bar. ....	41
Table 13 element dispersion of post run I-Cu foam at condition 5 bar. ....	42
Table 14 Element dispersion of post run I-Cu foam at condition 10 bar. ....	42
Table 15 Faradic efficiency of CO and ethylene for 20 min. (H <sub>2</sub> O 1 ml min <sup>-1</sup> and CO <sub>2</sub> 60 ml min <sup>-1</sup> ).....	43

## LIST OF FIGURES

	Page
Figure 1 Molecule of ethylene.....	6
Figure 2 Schematic illustration of electrophoretic deposition process. (a) Cathodic EPD and (b) anodic EPD.....	8
Figure 3 Faradaic efficiencies vs potential for Cu <sub>sph</sub> (200 μg/cm <sup>2</sup> ), Cu <sub>cub</sub> (250 μg/cm <sup>2</sup> ), and Cu <sub>oh</sub> (50 μg/cm <sup>2</sup> ) deposited on a GDL and measured in the gas-fed flow cell in 1 M KOH.....	9
Figure 4 SEM images of a,b) c-Cu <sub>2</sub> O, c,d) o-Cu <sub>2</sub> O, and e,f) t-Cu <sub>2</sub> O. ....	10
Figure 5 Faradic of ethylene value for c-Cu <sub>2</sub> O, o-Cu <sub>2</sub> O, and t-Cu <sub>2</sub> O as a function of the potential. ....	10
Figure 6 Structural characterization of defect CuO nanosheet (a-c).....	11
Figure 7 Electrochemical CO <sub>2</sub> ERR performance ethylene FE at various applied potentials for different catalysts.....	12
Figure 8 Effect of CO <sub>2</sub> pressure on the electrochemical reduction of CO <sub>2</sub> on a Cu electrode without stirring electrolyte of 0.1 mol dm <sup>-3</sup> KHCO <sub>3</sub> at 25°C. Current density: 163 mA cm <sup>-2</sup> . (○) Hydrocarbons, (●) H <sub>2</sub> , and (□) HCOOH. ....	13
Figure 10 block flow diagram for copper foam electrode preparation.....	16
Figure 11 CO <sub>2</sub> ERR Cell configuration.....	17
Figure 12 Block flow diagram of novel electrochemical tubular fixed bed reactor for CO <sub>2</sub> reduction to ethylene production .....	17
Figure 13 XRD patterns of fresh copper foam, ionomer copper foam and post run copper foam.....	19
Figure 14 SEM of Cu foam a) before and b) after CO <sub>2</sub> reduction and I-Cu foam c) before and d) after CO <sub>2</sub> reduction at 3 bar.....	20

Figure 15 The concentration of a) CO and b) ethylene from Cu foam and I-Cu foam at 3 bar. During the 120 min experiments, the following cell voltages were applied: 5 V for 60 min, 6 V for 30 min and 7 V for 30 min. ....	21
Figure 16 The current density for Cu foam and I-Cu foam at condition 3 bar. During the 120 min experiments, the following cell voltages were applied: 5 V for 60 min, 6 V for 30 min, and 7 V for 30 min. ....	22
Figure 17 Effect of ionomer (sustainion XA9) on the electrochemical reduction of CO <sub>2</sub> on Cu foam and I-Cu foam at 3 bar.....	23
Figure 18 The concentration of a) CO and b) ethylene from I-Cu foam at different pressure. During the 150 min experiments, the following cell voltages were applied: 5 V for 60 min, 6 V for 30 min and 7 V for 30 min. ....	24
Figure 19 The current for I-Cu foam at different pressure. During the 150 min experiments, the following cell voltages were applied: 5 V for 60 min, 6 V for 30 min, and 7 V for 30 min.....	25
Figure 20 Effect of pressure on the electrochemical reduction of CO <sub>2</sub> on I-Cu foam. ....	26
Figure 21 Effect of potential on the electrochemical reduction of CO <sub>2</sub> on I-Cu foam. ....	27
Figure 22 The concentration of a) CO and b) ethylene from I-Cu foam at different 60 ml min <sup>-1</sup> reactant gas. During the 150 min experiments, the following cell voltages were applied: 5 V for 60 min, 6 V for 30 min, 7 V for 30 min and 8 V for 30 min.....	28
Figure 23 XRD of copper powder .....	36
Figure 24 XRD of fresh Cu foam, I-Cu foam and post run I-Cu foam. ....	36
Figure 25 SEM of fresh Cu foam.....	37
Figure 26 SEM of fresh I-Cu foam. ....	37
Figure 27 SEM of fresh Cu-elec. ....	37
Figure 28 SEM of fresh Cu-ink.....	37

Figure 29 SEM of post run Cu foam at 3 bar.....	37
Figure 30 SEM of post run I-Cu foam at condition 3 bar.....	38
Figure 31 SEM of post run I-Cu foam at condition 5 bar.....	38
Figure 32 SEM of post run I-Cu foam at condition 10 bar.....	38
Figure 33 element dispersion of fresh Cu foam.....	39
Figure 34 SEM of fresh I-Cu foam.....	39
Figure 35 SEM of fresh Cu-elec.....	40
Figure 36 SEM of fresh Cu-ink.....	40
Figure 37 SEM of post run Cu foam at condition 3 bar.....	41
Figure 38 SEM of post run I-Cu foam at condition 3 bar.....	41
Figure 39 SEM of post run I-Cu foam at condition 5 bar.....	42
Figure 40 SEM of post run I-Cu foam at condition 10 bar.....	42
Figure 41 The concentration of a) CO and b) ethylene from Cu foam and I-Cu foam at 3 bar. During the 120 min experiments, the following cell voltages were applied: 5 V for 60 min, 6 V for 30 min and 7 V for 30 min.....	44
Figure 42 The current density for Cu foam and I-Cu foam at condition 3 bar. During the 120 min experiments, the following cell voltages were applied: 5 V for 60 min, 6 V for 30 min, and 7 V for 30 min.....	44
Figure 43 Effect of ionomer (sustainion XA9) on the electrochemical reduction of CO <sub>2</sub> on Cu foam and I-Cu foam at 3 bar.....	45
Figure 44 The concentration of a) CO and b) ethylene from I-Cu foam at different pressure. During the 150 min experiments, the following cell voltages were applied: 5 V for 60 min, 6 V for 30 min and 7 V for 30 min.....	45
Figure 45 The current for I-Cu foam at different pressure. During the 150 min experiments, the following cell voltages were applied: 5 V for 60 min, 6 V for 30 min, and 7 V for 30 min.....	46

Figure 46 Effect of pressure on the electrochemical reduction of CO <sub>2</sub> on I-Cu foam. .....	46
Figure 47 Effect of potential on the electrochemical reduction of CO <sub>2</sub> on I-Cu foam. .....	47
Figure 48 The concentration of a) CO and b) ethylene from I-Cu foam at different ml min <sup>-1</sup> reactant gas. During the 150 min experiments, the following cell voltages were applied: 5 V for 60 min, 6 V for 30 min, 7 V for 30 min and 8 V for 30 min.....	47
Figure 49 The current for I-Cu foam at different reactant gas. During the 150 min experiments, the following cell voltages were applied: 5 V for 60 min, 6 V for 30 min, and 7 V for 30 min.....	48



# CHAPTER 1

## INTRODUCTION

### 1.1 Background

Concentration of CO<sub>2</sub> in the atmosphere has increased by 30% since the industrial revolution and fossil fuel utilization. Excessive CO<sub>2</sub> in the atmosphere causes natural disasters such as rising global temperatures and rising sea levels. The main cause of this problem is the one-way injection of carbon from fossil fuels/resources into the atmosphere. However, banning their usage would also cut the supply of carbon sources for human civilization, unless processes for converting CO<sub>2</sub> to valuable products are in place. Many technologies for CO<sub>2</sub> utilization exist: reforming, hydrogenation, Biological conversion and carbon dioxide electrochemical reduction reaction (CO<sub>2</sub>ERR). CO<sub>2</sub>ERR is to convert CO<sub>2</sub> into carbon-containing products such as carbon monoxide (CO), methane (CH<sub>4</sub>), formic acid (HCOOH), methanol (CH<sub>3</sub>OH), ethylene (C<sub>2</sub>H<sub>4</sub>) and ethanol (C<sub>2</sub>H<sub>5</sub>OH) by proton and electron transfer [1, 2]. CO<sub>2</sub>ERR offers several means of control: electrode material, current density, applied voltage, electrolyte composition and concentrations. The reaction can also be carried out at ambient temperature and pressure, unlike other thermochemical methods in which elevated temperature and pressure are virtually always required. There are 2 main reactions. First, water is oxidized to oxygen at an anode call “oxygen evolution reaction (OER)”. Second, CO<sub>2</sub>ERR occurs at cathode and product production depend on cathode catalyst or material. Moreover, Hydrogen evolution reaction concomitant occurs at cathode.

Traditional electrochemical CO<sub>2</sub>ERR is performed in divided electrochemical cells. An ion-exchange membrane is used to form 2 chambers in an electrochemical cell so that carbon products from the cathode are not mixed with oxygen from the anode. Nevertheless, pressurization in this type of cell is

difficult in practice. An excessive pressure difference between the anode and cathode chambers can lead to membrane rupture. Furthermore, CO<sub>2</sub> transport from the cathode chamber to the anode chamber in the form of bicarbonate through an anion-exchange membrane, which is commonly used, is somewhat unavoidable, leading to decreased single-pass conversion.

In this work, we design and study a single-chamber tubular fixed-bed electrochemical reactor for CO<sub>2</sub>ERR that is not affected by the two problems described earlier. Nonetheless, the single-chamber design allows carbon products and oxygen to come into contact and presents risk of explosion. However, it may be useful for conversion of heavily diluted CO<sub>2</sub> sources such as flue gases; the existence of inert N<sub>2</sub> put the gas composition outside the flammability limits. In this application, purification of CO<sub>2</sub> is not needed and hence its cost may be eliminated.

Ethylene is a raw material used in manufacture of polymers such as polyethylene terephthalate (PET), polyethylene, polyvinylchloride (PVC) and polystyrene (PS). For high ethylene production, copper is probably the only metal which can produce C<sub>2+</sub> compounds by multielectron reaction [1-4]. In addition, copper-based catalysts have unique properties among metal catalysts for electrochemical reduction of CO<sub>2</sub> to fuel or hydrocarbons. However, the practical application of Cu-based catalyst in the CO<sub>2</sub>ERR still faces problems such as low current density, poor stability and poor selectivity. Therefore, developing efficient process conditions to achieve high current densities, selectivity and stability would very likely affect the feasibility of CO<sub>2</sub>ERR technology.

In this study, Copper foam (Cu foam) and ionomer copper foam (I-Cu foam) will be employed in our single-chamber reactor. The Cu foam and I-Cu foam are then used as a cathode in the electrochemical tubular fixed bed reactor for continuous conversion of CO<sub>2</sub> to ethylene to observe the catalyst's selectivity and activity. the performance of CO<sub>2</sub>ERR is improved by increasing pressure and cell voltage.



## 1.2 Research objective

1.2.1 To study electrochemical CO<sub>2</sub>ERR with Copper cathode in electrochemical tubular fixed-bed reactor.

1.2.2 To study the effects of Copper cathode preparation methods on CO<sub>2</sub>ERR in electrochemical tubular fixed-bed reactor.

1.2.3 To study effects of pressures and applied cell voltage on electrochemical CO<sub>2</sub>ERR in electrochemical tubular fixed-bed reactor.

## 1.3 Scope of study

1.3.1 Electrochemical CO<sub>2</sub>ERR performed in an electrochemical tubular fixed bed reactor.

1.3.2 Effects of cell potential and pressure.

## 1.4 Expected benefit

1.4.1 A prototype of single-chamber electrochemical tubular fixed bed reactor for electrochemical conversion of diluted CO<sub>2</sub> into ethylene.

## CHAPTER 2

### THEORY and LITERATURE REVIEWS

#### 2.1 Theory

##### 2.1.1 Electrochemical CO<sub>2</sub> reduction reaction (CO<sub>2</sub>ERR)

CO<sub>2</sub>ERR has been investigated to decrease concentration of CO<sub>2</sub> in atmosphere to value-added chemicals by proton and electron transfer. The product from CO<sub>2</sub>ERR is depending on active metal catalyst. Moreover, Morphology, pH, Electrolyte and structure have effect to produce products. The products from CO<sub>2</sub>ERR is considered by (1) Chemical adsorption of CO<sub>2</sub> on the surface of a catalyst (cathode). (2) Electron transfer and/or proton migration to break C–O bonds and/or form C–H bonds. (3) Rearrangement of product species followed by desorption from electrode surface and diffusion into electrolyte [5].

In general, the cell of electrochemical CO<sub>2</sub>ERR consists of cathodic compartment, where the reduction process is governed by a multi-step-based coordination chemistry comprising two, six, eight, and twelve electrons for the formation of the common products CO, CH<sub>3</sub>OH, CH<sub>4</sub>, and C<sub>2</sub>H<sub>4</sub>, respectively as shown in table 1., and anodic compartment, where oxygen evolution occurs and produces acidic condition on electrode. Accordingly, an electrode of anode should resist and be stable in acidic condition such as Titanium (Ti) and Platinum (Pt). The two compartments are separated by membrane, which has a role of protecting “short circuit” and provides the ionic conduction for allowing the current flow through the system.

Table 1 The chemical equation and the corresponding standard electrode potential (V vs. SHE)[1, 6-8].

Half electrochemical thermodynamic reaction	V vs. SHE	Eq.
$\text{CO}_2(\text{g}) + 2\text{H}^+ + 2\text{e}^- \rightleftharpoons \text{CO}(\text{g}) + \text{H}_2\text{O}(\text{l})$	- 0.106	1
$\text{CO}_2(\text{g}) + 2\text{H}_2\text{O}(\text{l}) + 2\text{e}^- \rightleftharpoons \text{CO}(\text{g}) + 2\text{OH}^-$	- 0.934	2
$\text{CO}_2(\text{g}) + \text{H}^+ + 6\text{e}^- \rightleftharpoons \text{CH}_3\text{OH}(\text{l}) + \text{H}_2\text{O}(\text{l})$	0.016	3
$\text{CO}_2(\text{g}) + 5\text{H}_2\text{O}(\text{l}) + 6\text{e}^- \rightleftharpoons \text{CH}_3\text{OH}(\text{l}) + 6\text{OH}^-$	- 0.812	4
$\text{CO}_2(\text{g}) + 8\text{H}^+ + 8\text{e}^- \rightleftharpoons \text{CH}_4(\text{g}) + 2\text{H}_2\text{O}(\text{l})$	0.169	5
$\text{CO}_2(\text{g}) + 6\text{H}_2\text{O}(\text{l}) + 8\text{e}^- \rightleftharpoons \text{CH}_4(\text{g}) + 8\text{OH}^-$	- 0.659	6
$2\text{CO}_2(\text{g}) + 12\text{H}^+ + 12\text{e}^- \rightleftharpoons \text{CH}_2\text{CH}_2(\text{g}) + 4\text{H}_2\text{O}(\text{l})$	0.064	7
$2\text{CO}_2(\text{g}) + 8\text{H}_2\text{O}(\text{l}) + 12\text{e}^- \rightleftharpoons \text{CH}_2\text{CH}_2(\text{g}) + 12\text{OH}^-$	- 0.764	8

CO<sub>2</sub>ERR is alternative method for CO<sub>2</sub> transforming to hydrocarbon and alcohol, that has advantages 1. The parameters during electrochemical synthesis can be easily and precisely controlled, including the reaction electrode, current density, applied voltage, electrolyte composition and concentrations 2. The preparation process is under mild conditions (at ambient temperature and pressure) 3. Electricity can be provided through renewable energy sources (solar, wind, tidal, etc.) without generating any new sources of carbon dioxide[1, 9].

### 2.1.2 Ethylene

Ethylene (Fig. 1) is a widely raw material used in the manufacture of polymers (e.g. packaging, automotive and electrical applications). Furthermore, as compared to C<sub>1+</sub>, the C<sub>2+</sub> product has a greater market price. For high ethylene production, Copper is the only special metal that can produce C<sub>2+</sub> compounds by multielectron reaction [1-4]. In addition, Cu-based catalyst has unique properties among metal catalyst has

been considered as a material for electrochemical reduction of CO<sub>2</sub> to fuel or hydrocarbon.

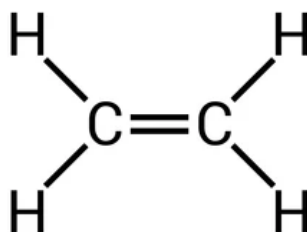


Figure 1 Molecule of ethylene

### 2.1.3 Active metal

Various catalysts have been studied for the CO<sub>2</sub>ERR such as pure material, metal alloys and inorganic compounds (metal oxide, sulfides, etc.) in electrolytes (primarily 0.1M KHCO<sub>3</sub>). They can be divided into four groups based on the principal reduction product: (i) Cu, the only metal that is reducing CO<sub>2</sub> to hydrocarbon, alcohol and other carbon containing chemicals at a significant rate; (ii) Au, Ag, Zn, Pd and Ga, from which CO is the major product; (iii) Pb, In, Sn and Bi, primary producing formate; (iv) Ni, Fe, Pt, and Ti, where only hydrogen evolution, but no CO<sub>2</sub> reduction, is observed at steady state. The CO<sub>2</sub> reduction capability of the metals in groups *i* and *ii* is attributed to the stabilization of \*CO<sub>2</sub><sup>-</sup> and/or \*COOH (\* denotes a surface adsorption site) on their surfaces, whereas the formation of formate on group *iii* metals is believed to occur via hydration of nonadsorbing CO<sub>2</sub><sup>-</sup>. Group *iv* metals are believed to bind to the intermediate \*CO too strongly, which inhibits the continual reduction of CO<sub>2</sub>, leaving only the evolution of hydrogen from the interstitial sites among adsorbed CO. [1-4, 9, 10].

### 2.1.4 Electrophoretic deposition

Electrophoretic deposition (EPD) is a colloidal technique used in ceramic manufacture that offers the following advantages: fast formation time, simple

apparatus, no substrate shape constraint, and no need for binder burnout because the green coating includes few or no organics. The EPD method, in comparison to other advanced shaping processes, is particularly adaptable since it can be quickly adjusted for a given purpose. With just modest changes in electrode design and positioning, deposition may be done on a flat, cylindrical, or any other shaped substrate. Despite the fact that it is a wet process, EPD allows for simple control of the thickness and shape of deposited films by adjusting the deposition duration and applied potential. When a DC electric field is applied to charged powder particles distributed or suspended in a liquid media, they are attracted and deposited onto a conductive substrate of opposite charge. The term "electrodeposition" is often used interchangeably to refer to either electroplating or electrophoretic deposition, however it is more commonly used to refer to the former. The contrast between the two processes is seen in Table 2. Depending on which electrode the deposition happens on, EPD can be one of two forms of electrophoretic deposition. Deposition occurs on the cathode when the particles are positively charged, and the process is known as cathodic electrophoretic deposition. Anodic electrophoretic deposition is the deposition of negatively charged particles on a positive electrode (anode). Any of the two modes of deposition can be achieved by modifying the surface charge on the particles. The two electrophoretic deposition processes are shown schematically in Fig. 2. [11].

จุฬาลงกรณ์มหาวิทยาลัย  
CHULALONGKORN UNIVERSITY

Table 2 Characteristics of electrodeposition techniques.[11]

Property	Electroplating	Electrophoretic deposition
Moving species	Ions	Solid particles
Charge transfer on deposition	Ion reduction	None
Required conductance of liquid medium	High	Low
Preferred liquid	Water	Organic

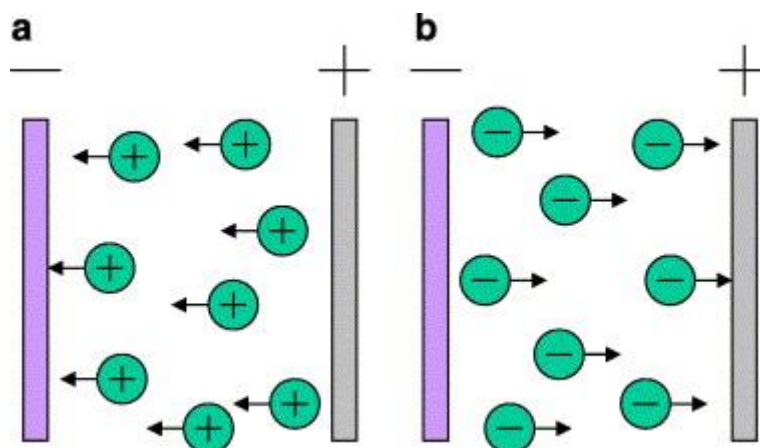


Figure 2 Schematic illustration of electrophoretic deposition process. (a) Cathodic EPD and (b) anodic EPD.

## 2.2 Literature reviews

This part focus on ethylene production in gas phase. First, The Cu-based catalyst cathode were synthesized by synthesis route. Second, The performance of Cu-based catalyst cathode in reactor for ethylene production. Moreover, facet, potential, and pressure are considered.

Copper based catalyst has been studied about selectivity and activity for CO<sub>2</sub> reduction by conduct relationship between structure and performance such as crystal plane, size, morphology and defect.

### 2.2.1 Facets effect

Different copper facets exhibit different performance and intermediate reactions. For example, Hori et al. [12, 13] purposed that Cu(100) surfaces mostly produce C<sub>2</sub>H<sub>4</sub> with a small amount of CH<sub>4</sub>, whereas Cu(110) and Cu(111) surfaces primarily form CH<sub>4</sub> with very small C<sub>2</sub>H<sub>4</sub>. the electrochemical reduction of CO<sub>2</sub> to CH<sub>4</sub> and C<sub>2</sub>H<sub>4</sub> from aqueous solutions at copper foil electrodes with high current efficiencies

Gian Luca De Gregorio et al. [3] study investigated physical on Cu single crystals in an H-cell. The catalytic performances were tested in a gas-fed flow cell

with 1M KOH as supporting electrolyte. Faradic efficiency of each product vs potential for morphology report in Fig. 3, when compared to the  $\text{Cu}_{\text{sphere}}$  catalysts of the potential, the  $\text{Cu}_{\text{cubic}}$  catalysts had a greater selectivity for ethylene. The conversion of  $\text{CO}_2$  to ethylene in the (100) facets ranged from 55 percent at 100  $\text{mA}/\text{cm}^2$  and  $-0.65$  vs RHE to around 60 percent at 200  $\text{mA}/\text{cm}^2$  and  $-0.7\text{V}$  vs RHE. Methane was the major product of  $\text{Cu}_{\text{octahedral}}$  catalysts. At 100  $\text{mA}/\text{cm}^2$  and  $-0.91\text{V}$  versus RHE, the greatest FE was 53%. With the least amount of  $\text{H}_2$  output. Ethylene is also available as a product, although only with a conversion efficiency of 10%.

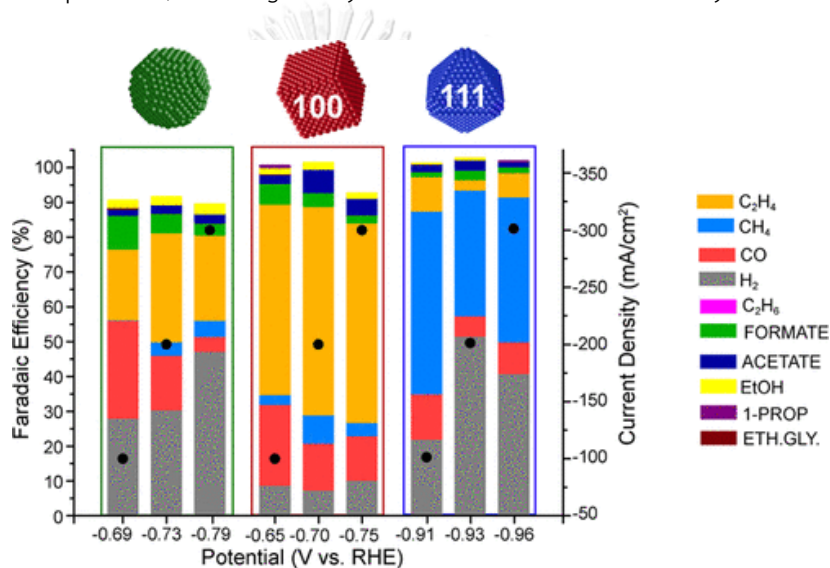


Figure 3 Faradaic efficiencies vs potential for  $\text{Cu}_{\text{sph}}$  ( $200 \mu\text{g}/\text{cm}^2$ ),  $\text{Cu}_{\text{cub}}$  ( $250 \mu\text{g}/\text{cm}^2$ ), and  $\text{Cu}_{\text{oh}}$  ( $50 \mu\text{g}/\text{cm}^2$ ) deposited on a GDL and measured in the gas-fed flow cell in 1 M KOH.

Yugang Gao et al. [3] study effect of morphology of  $\text{Cu}_2\text{O}$  such as cubic (c) with {100}, Octahedral (o) with {111}, and truncated-octahedral (t) with both {100} and {111} to  $\text{CO}_2$  reduction in H-type cell. Morphology  $\text{Cu}_2\text{O}$  catalysts were synthesized by wet chemical method. Polyvinylpyrrolidone (PVP) (0g for c, 4g for o, and 6g for t),  $\text{CuCl}_2 \cdot 2\text{H}_2\text{O}$ , and NaOH were mixed for 30 min. after stirred, ascorbic acid was added in solution and continuously stirred for 3 h. The mixture solution was aged in water bath at  $55 \text{ }^\circ\text{C}$ . then, all products were precipitated by centrifuge for

removing liquid solution. The morphology as prepared were characterized by scanning electron microscopy (SEM) that shown in Fig 4. The result show activity and selectivity of morphology's effects on  $\text{CO}_2$  reduction were in Fig. 5.  $\text{C}_2\text{H}_4$  production increased in order,  $c\text{-Cu}_2\text{O} < o\text{-Cu}_2\text{O} < t\text{-Cu}_2\text{O}$  (with FE38%, 45% and 59%, respectively).

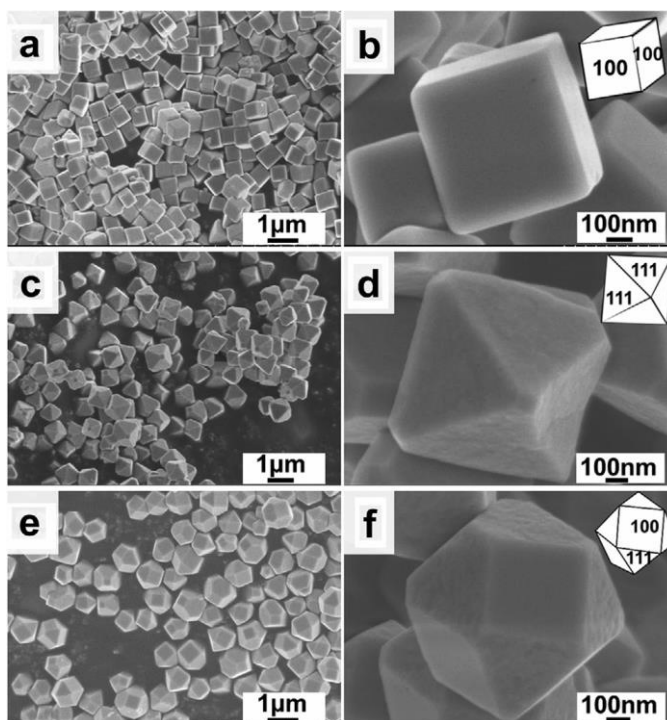


Figure 4 SEM images of a,b)  $c\text{-Cu}_2\text{O}$ , c,d)  $o\text{-Cu}_2\text{O}$ , and e,f)  $t\text{-Cu}_2\text{O}$ .

CHULALONGKORN UNIVERSITY

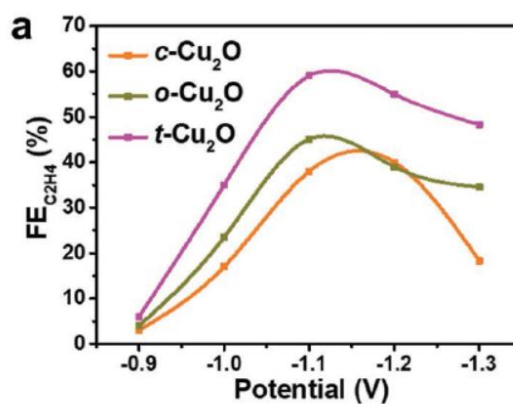


Figure 5 Faradic of ethylene value for  $c\text{-Cu}_2\text{O}$ ,  $o\text{-Cu}_2\text{O}$ , and  $t\text{-Cu}_2\text{O}$  as a function of the potential.



### 2.2.2 Defect effect

The defects, are caused by vacancies, dislocations, surface strain, and grain boundary, can improved CO<sub>2</sub> reduction performance. First, the defects can affect the surface properties and optimize the binding energy or adsorption energy of reaction intermediates, and reaction pathway. Secondly, defects can change the reaction environment and increase the number of active sites to promote the reduction reaction [7].

Bingxing, Jianline et al. [14] investigated ethylene production from CO<sub>2</sub> on nanodefective Cu nanosheets. The nano defect Cu nanosheet (n-CuNS) were prepared by reduction method for CuO nanosheet. Figure 6 shows the pits are ~2-14 nm. For comparison performance between with/without defect copper nanosheet (CuNS) in CO<sub>2</sub>ERR, the current density at -1.18 V vs RHE on n-CuNS is 6 times higher than CuNS. The ethylene faradic efficiency over n-CuNS maintains values of >60% in a wide potential range of -0.88 to -1.48 V vs RHE. A maximum ethylene FE of 83.2% can be achieve at -1.18 V vs RHE as shown in figure 7.

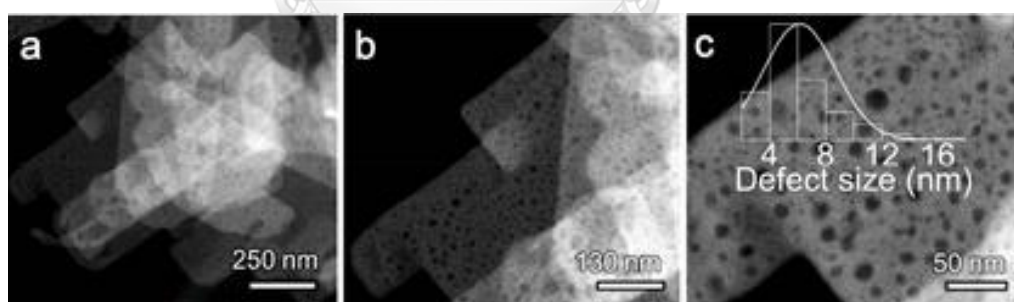


Figure 6 Structural characterization of defect CuO nanosheet (a-c).

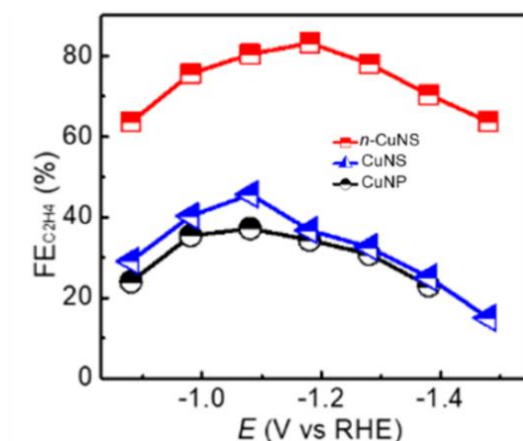


Figure 7 Electrochemical CO<sub>2</sub>ERR performance ethylene FE at various applied potentials for different catalysts.

### 2.2.3 Pressure

The other challenge is conversion rate that limited by the poor solubility of CO<sub>2</sub> in aqueous electrolyte (The concentration of CO<sub>2</sub> in aqueous solutions at 1 atm is 0.033 mol dm<sup>-3</sup>). From the Henry's Law, it is understood that increasing the concentration of dissolved CO<sub>2</sub> in the electrolyte can be achieved by decreasing temperature or increasing pressure.

Kohjiro Hara et al. [15] investigate hydrocarbon production in electrochemical reduction on Cu electrode by increasing CO<sub>2</sub> pressure. The results demonstrate that CO<sub>2</sub> reduction efficiencies are low at low CO<sub>2</sub> pressures, and the principal product is H<sub>2</sub> produced by water reduction. The efficiency of H<sub>2</sub> production decreases as CO<sub>2</sub> pressure rises, and hydrocarbons become the main product. When the CO<sub>2</sub> pressure is increased further, the production efficiency for HCOOH and/or CO is increased as seen in Fig. 8. Recep Kas et al. [2] study the process conditions in CO<sub>2</sub> electroreduction for hydrocarbon selectivity. CO<sub>2</sub> pressure, local CO concentration, and CO surface coverage are all higher. The increase in the amount of adsorbed CO from the surface as pressure rises reflects this as well.

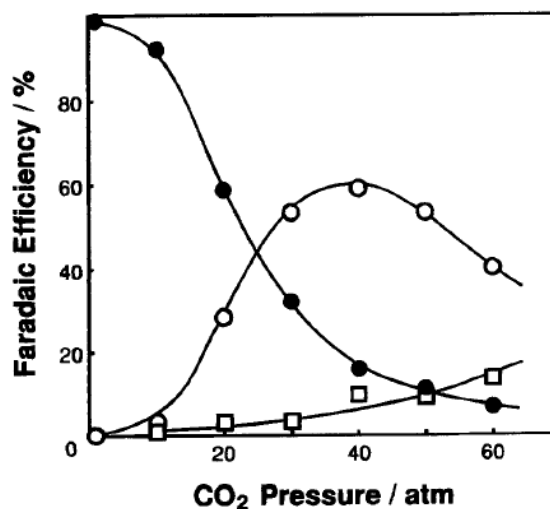


Figure 8 Effect of CO<sub>2</sub> pressure on the electrochemical reduction of CO<sub>2</sub> on a Cu electrode without stirring electrolyte of 0.1 mol dm<sup>-3</sup> KHCO<sub>3</sub> at 25°C. Current density: 163 mA cm<sup>-2</sup>. (○) Hydrocarbons, (●) H<sub>2</sub>, and (□) HCOOH.

#### 2.2.4 Electrolyte

Electrolyte can impact on the CO<sub>2</sub>ERR performance. There are one more factor that have complex relations with local environment on surface such as pH, buffer electrolyte and interaction of proton donor. The pH of electrolyte is concern to the activity because CO<sub>2</sub> can react with the electrolyte or by-product leading to increase local pH by HCO<sub>3</sub><sup>-</sup> and CO<sub>3</sub><sup>2-</sup> produced. Hori et al investigate selectivity of CH<sub>4</sub> and C<sub>2</sub>H<sub>4</sub> at cathode in pH dependent. The result show FE of ethylene is greater, when pH is increased by type of electrolyte, as show in table 3 [16]. The CO reduction has a mechanism pathway for CH<sub>4</sub> and C<sub>2</sub>H<sub>4</sub> formation. Xinyi Chen et al. investigate conversion of CO<sub>2</sub> to ethylene The FE for ethylene production reaches from 72% to 87% at a cathode potential of -0.47 V in 1 to 10 M KOH.

Table 3 Faradaic Efficiencies of Various Products from the Electroreduction of CO at a Cu Electrode in Aqueous Solutions. [16]

Electrolyte	pH	FE / %						
		CH <sub>4</sub>	C <sub>2</sub> H <sub>4</sub>	EtOH	n-PrOH	HCHO	H <sub>2</sub>	Total
Phosphate	6.0	16.80	1.70	0.00	0.00	0.02	75.40	93.90
KHCO <sub>3</sub>	9.6	16.20	5.50	2.70	0.30	0.03	65.40	90.10
KOH	12.9	1.00	14.10	5.80	1.10	0.05	70.70	92.80



## CHAPTER 3

### EXPERIMENTAL

This research study effect of CO<sub>2</sub> pressure and the potential for CO<sub>2</sub> reduction in an electrochemical tubular fixed-bed reactor. The products were detected and analyzed by Gas chromatography and an Infrared gas analyzer. However, the main product is ethylene gas.

#### 3.1 Chemicals and Materials

- 3.1.1 Copper foam
- 3.1.2 Graphite felt
- 3.1.3 sustainion XA-9 in 5% ethanol
- 3.1.4 Au wire (99.99%)
- 3.1.5 Nafion solution
- 3.1.6 Platinize Ti mesh
- 3.1.8 Carbon Black
- 3.1.9 2-isopropanol

## 3.2 Methodology

### 3.2.1 Preparation of copper electrodes

#### 3.2.1.1 Preparation of copper foam electrodes with/without ionomer.

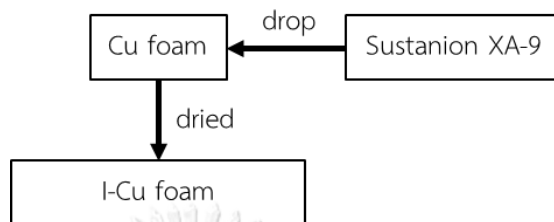


Figure 9 block flow diagram for copper foam electrode preparation.

From fig.10, 200  $\mu\text{L}$  of sustanion are dropped on copper foam (diameter 1.4 cm), then dry with air. The electrode is called “I-Cu foam”.

### 3.2.2 Preparation of an electrochemical $\text{CO}_2\text{ERR}$ cell

A cell for electrochemical  $\text{CO}_2\text{ERR}$  consists of 3 main parts. Cu foam and I-Cu foam is used as the cathode. Pieces of platinized Ti mesh are used as current collectors and the anode. Additional pieces of graphite felt are used to provide compression for firm electrical contacts between cell components. A bed of ion-exchange resin (Amberlite IRA-402) is placed between the cathode and anode as an electrolyte. Fig.12. shows the configuration of these cell components.

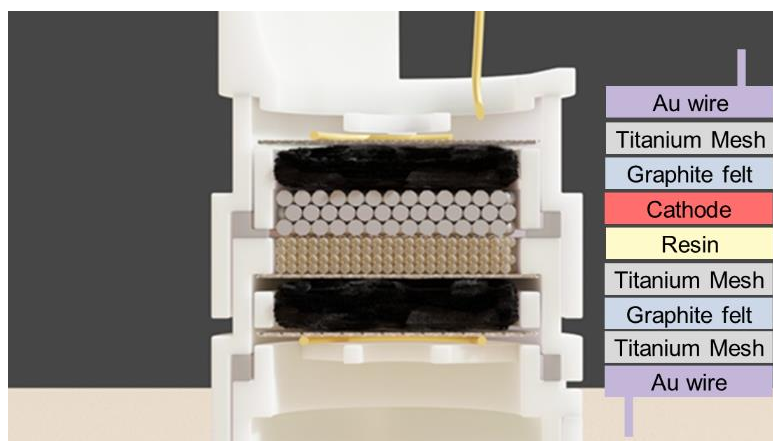


Figure 10 CO<sub>2</sub>ERR Cell configuration

### 3.2.3 Electrochemical measurements

High-purity CO<sub>2</sub> gas is fed continuously to the electrochemical tubular fixed bed reactor. A mass flow controller is installed to control the flow rate. Deionized water is saturated with CO<sub>2</sub> in the water drum and driven to the reactor by the pressurized CO<sub>2</sub>. A needle valve is installed to control the flow rate of the water; only a low flow rate is needed just to moisten the ion-exchange resin so that its electrical conductivity is sustained. The reaction contains a CO<sub>2</sub> flow rate of 60 ml min<sup>-1</sup> and a CO<sub>2</sub>-saturated water flow rate of H<sub>2</sub>O 1 ml min<sup>-1</sup>. The products are detected and analyzed by Gas Chromatography (GC-2014) and Infrared Gas Analyzer (Model IR200, YOKOKAWA) in real time. Fig.13. illustrates the reactor system used in this work.

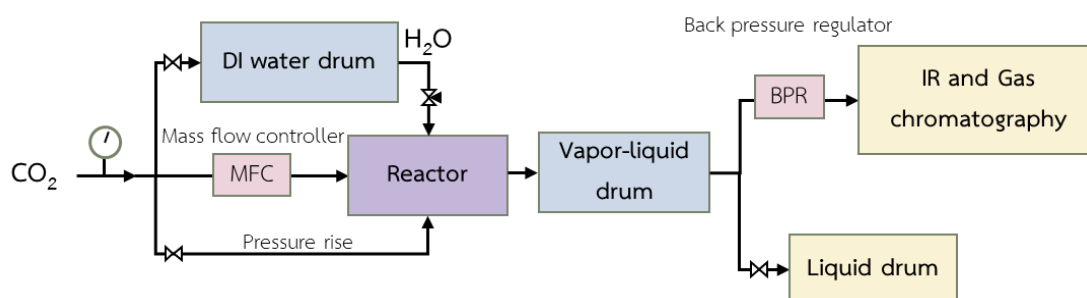


Figure 11 Block flow diagram of novel electrochemical tubular fixed bed reactor for CO<sub>2</sub> reduction to ethylene production

### 3.2.5 Characterization and Product analysis

SEM-EDX (Scanning electron microscopy with Energy Dispersive X-Ray) is a technology that uses an electron beam to scan the surface. The electron beam interacts with the material, resulting in a multitude of signals that may be used to identify a catalyst surface. EDX might also be used to describe and measure elemental composition.

X-Ray Diffraction (XRD) is a method that uses X-rays to diffract into a specified angle to characterize crystal structure and crystallite size.

A product from CO<sub>2</sub>ERR in electrochemical packed bed reactor are analyzed by Gas chromatography and IR for identification and measuring products concentration.

The Current from CO<sub>2</sub>ERR in electrochemical packed bed reactor could calculate Faradaic efficiency of CH<sub>4</sub> product by Eq. (9).

$$FE\% = \frac{\text{Number of electrons requires for reducing CO}_2 \text{ to product}}{\text{Total number of moles of electrons passed}} = \frac{y \int_0^t n \, dt \, F}{\int_0^t I \, dt} \quad (9)$$

When,

- y = Stoichiometric coefficient of electron required in table 1
- n = Number of moles of product produced
- F = Faraday constant (96,485.3329 s A mol<sup>-1</sup>)
- I = Electric current (A)
- t = time (s)



## CHAPTER 4

### RESULTS and DISCUSSIONS

An electrochemical tubular fixed-bed reactor was developed by scaling up for CO<sub>2</sub> reduction in the gas phase for ethylene production. The effect of cathode preparation, CO<sub>2</sub> pressure (3, 5, and 10 bar), and potential (5, 6, and 7 V) were investigated. There were two forms of cathode: commercial copper foam (Cu foam) and ionomer copper foam (I-Cu foam). The behavior of CO and C<sub>2</sub>H<sub>4</sub> was observed using Gas Chromatography (GC-2014) and an Infrared Gas Analyzer (Model IR200, YOKOKAWA).

#### 4.1 Characterization of Cu foam electrodes

The diffractogram of copper electrode (fig.14) shows characteristic diffraction peaks (111), (200), and (220) of Cu at 2theta values of 43.3°, 50.4°, and 74.1°, respectively, according to JCPDS-ICDD ref. 004-0836. The crystallite size of CU foam, I-Cu foam, and post run I-Cu foam calculated by Scherrer's equation from this XRD pattern is 24.20, 26.08, and 28.02 nm, respectively.

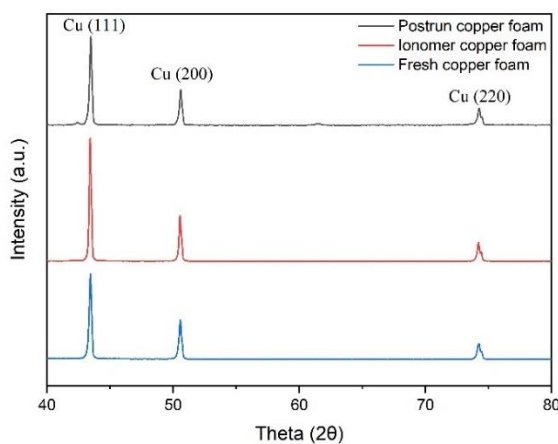


Figure 12 XRD patterns of fresh copper foam, ionomer copper foam and post run copper foam

The surface of Cu foam and I-Cu foam before and after CO<sub>2</sub> reduction were examined by SEM. From fig.15, the surface of Cu foam and I-Cu foam after CO<sub>2</sub> reduction are rough when compared with before the CO<sub>2</sub>ERR. There is also unexpected formation of possibly cubic particles, which may also be Cu. Nevertheless, this matter has not been pursued further. In addition, Stefan Popović et al reported densely packed 6 nm spherical Cu nanoparticles undergo a structural transformation into electrocatalytically active cubic particles and doesn't affect to performance of C<sub>2</sub> and C<sub>3</sub> production from CO<sub>2</sub> reduction for 10 h [17].

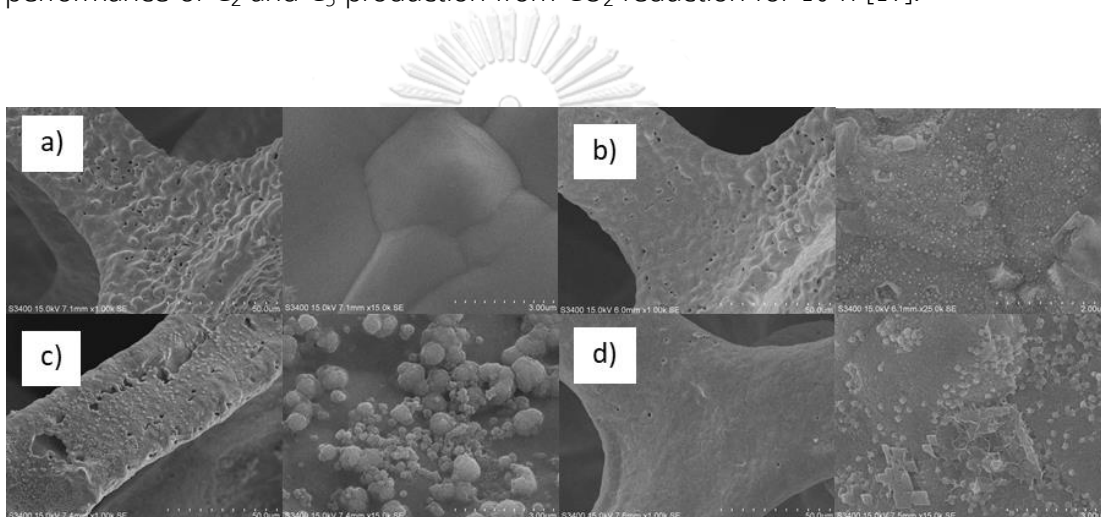


Figure 13 SEM of Cu foam a) before and b) after CO<sub>2</sub> reduction and I-Cu foam c) before and d) after CO<sub>2</sub> reduction at 3 bar.

#### 4.2 Effects of ionomer (Sustainion XA-9) coating on Cu foam

The results from the electrochemical reduction of CO<sub>2</sub> at 3 bar with a CO<sub>2</sub> flow rate of 60 ml min<sup>-1</sup> and a trickling rate of CO<sub>2</sub>-saturated water of 1 ml min<sup>-1</sup> are shown in fig 16-18. The cell voltages applied during the 120 min experiment were as follows: 5 V for 60 min, 6 V for 30 min, and 7 V for 30 min. Fig 16 shows the concentrations of CO and ethylene from the reactor. At this pressure, ethylene concentrations were < 20 ppm but that from I-Cu foam was clearly higher. Ethylene concentrations appeared to increase gradually during the application of 5 V cell

voltage and then decrease gradually at higher cell voltages. The concentrations of CO were clearly higher with a peak CO concentration from the I-Cu foam. The overall trends were similar to those of ethylene concentrations.

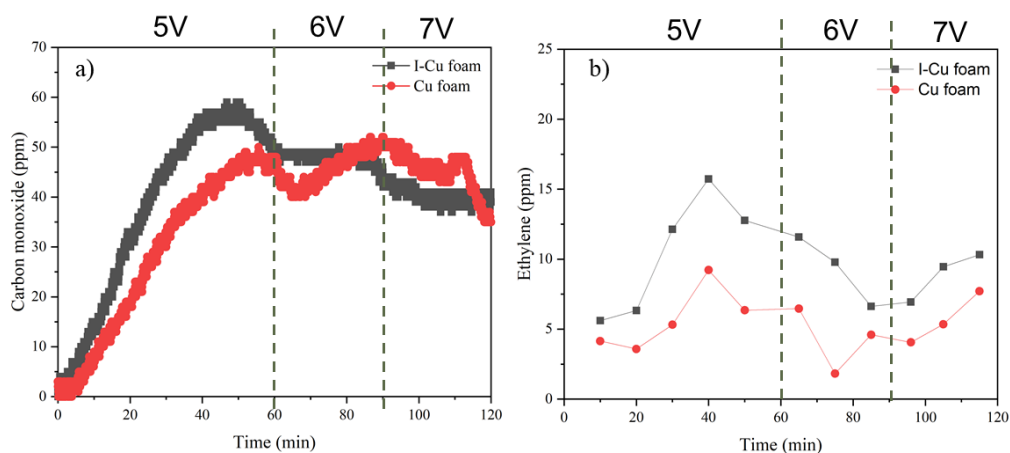


Figure 14 The concentration of a) CO and b) ethylene from Cu foam and I-Cu foam at 3 bar. During the 120 min experiments, the following cell voltages were applied: 5 V for 60 min, 6 V for 30 min and 7 V for 30 min.

Fig 17 shows the currents from the applied cell voltages during the 120 min experiment. The currents from the two types of electrodes were close to one another and had similar trends. At 7 V, the currents appeared to increase somewhat abruptly and then fall steadily. In addition, an increase in the current as the cell voltage increased did not appear to be exponential. This suggests that the main resistance of the cell was from the electrolyte, i.e. the 2 mm thick resin bed, which is not designed by the manufacturer to be used as an electrolyte.

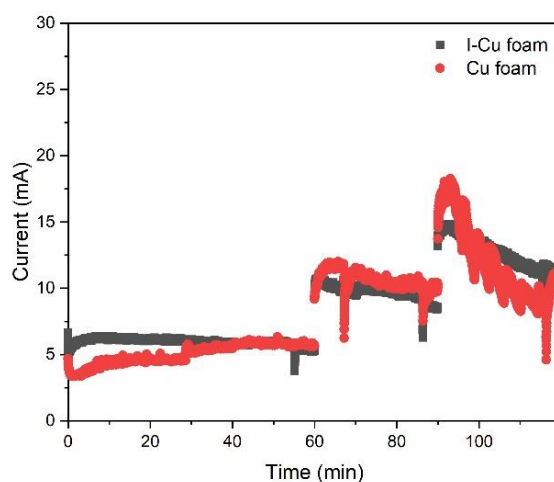


Figure 15 The current density for Cu foam and I-Cu foam at condition 3 bar. During the 120 min experiments, the following cell voltages were applied: 5 V for 60 min, 6 V for 30 min, and 7 V for 30 min.

Fig 18 compares the faradaic efficiencies of ethylene and CO from Cu foam and I-Cu foam electrodes at different applied cell voltages. At 5 V, the faradaic efficiencies of ethylene were higher than those of CO despite the lower ethylene concentrations shown in Fig 16 because they reduction to ethylene and CO requires 12 and 2 mol of electrons, respectively, per 1 mol of product. The faradaic efficiencies of both products were comparable to their counterparts at cell voltages of 5 V but dropped significantly at 6 and 7 V. This was consistent with the lower CO and ethylene concentrations at higher cell voltages previously shown in fig 16 and the higher total currents in fig 17. Lower faradaic efficiencies of the two products are believed to be mainly caused by an increase in the H<sub>2</sub> evolution rate concomitant to any aqueous systems.

The faradaic efficiencies of both products from I-Cu foam were higher than those from Cu foam. This indicates that Sustainion XA-9 increased faradaic efficiencies for the formation of the two products. The ionomer might selectively

suppress to the formation of ethylene because of the distribution and content of ionomer can directly influence the protonic and electronic conductivity of the catalyst layer [18]. The mechanism plausibly involved modification of electrode surface pH. Without the ionomer, the surface pH at the Cu foam was supposedly low (3-4) as it was covered with a layer of  $\text{CO}_2^-$  saturated water without any added salts. With the anion-exchange ionomer, the electrode coating converted  $\text{CO}_2$  with the absorbed  $\text{OH}^-$  into  $\text{HCO}_3^-$  and  $\text{CO}_3^{2-}$  [19] and possibly raised the surface pH to 7-8.

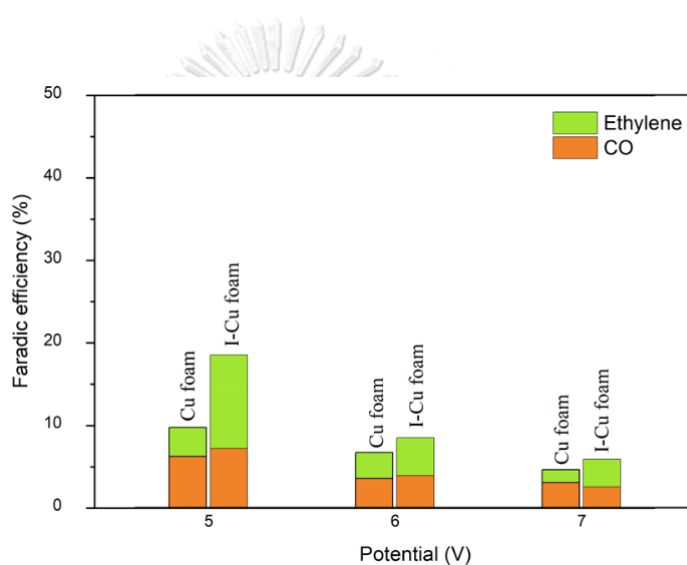


Figure 16 Effect of ionomer (sustainion XA9) on the electrochemical reduction of  $\text{CO}_2$  on Cu foam and I-Cu foam at 3 bar.

### 4.3 Effect of pressure

The results from the electrochemical reduction of  $\text{CO}_2$  at 3, 5 and 10 bar with a  $\text{CO}_2$  flow rate of  $60 \text{ ml min}^{-1}$  and a trickling rate of  $\text{CO}_2$ -saturated water of  $1 \text{ ml min}^{-1}$  are shown in fig 19-21. The cell voltages applied during the 120 min experiment were as follows: 5 V for 60 min, 6 V for 30 min, and 7 V for 30 min. Fig.19 shows the concentration of CO and ethylene from reactor. CO concentration were  $>40 \text{ ppm}$  3 bar. Ethylene concentration were highest at 10 bar. Concentration of

ethylene and CO were otherwise trended because CO intermediate was used for CO<sub>2</sub> transformation to ethylene when pressure was increased.

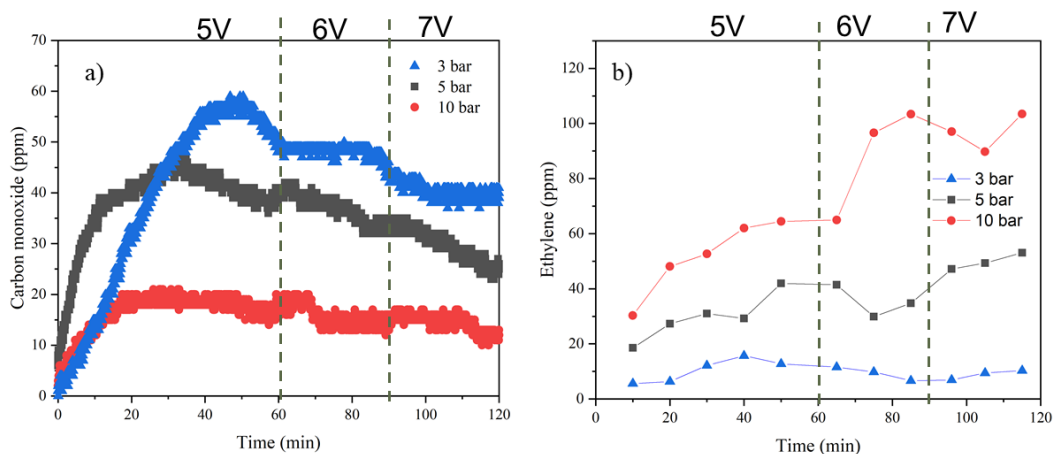


Figure 17 The concentration of a) CO and b) ethylene from I-Cu foam at different pressure. During the 150 min experiments, the following cell voltages were applied: 5 V for 60 min, 6 V for 30 min and 7 V for 30 min.

Fig 20 shows the currents from the applied cell voltages during the 150 min experiment. The currents from the different pressure were increased meanwhile ethylene concentration were increased and CO concentration were decreased. So, the number of electrons introduced is utilized to adsorb CO intermediate on the surface and transform to ethylene. At 10 bar, the current was lower than at 5 bar but ethylene concentration was higher than 3 and 5 bar. In addition, CO molecules adsorbed on the electrode surface suppress H<sub>2</sub> production, resulting in a decrease in the current density [20-22].

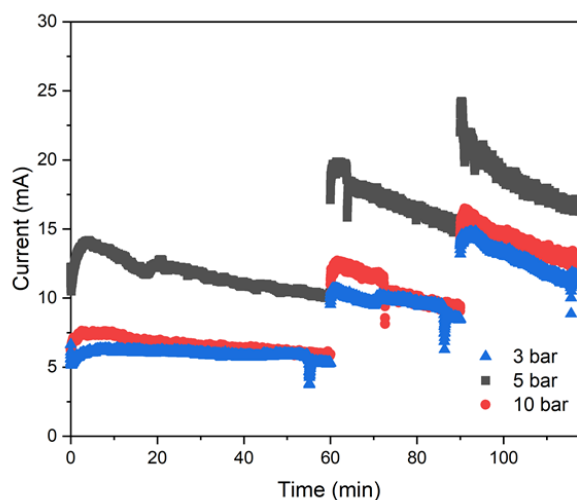


Figure 18 The current for I-Cu foam at different pressure. During the 150 min experiments, the following cell voltages were applied: 5 V for 60 min, 6 V for 30 min, and 7 V for 30 min.

Fig.21 compares the faradic efficiency of CO and ethylene at 3, 5 and 10 bar and different applied voltage. At 5 V with 3, 5, and 10 bar, faradic efficiency of  $C_2H_4$  was 11.34, 14.07, and 45.13 %, respectively. And faradic efficiency of CO was 7.16, 3.89, and 2.30 %, respectively. When increasing  $CO_2$  pressure, faradic efficiency of both products was kept to pointing the same thing. Faradic efficiency of ethylene gas was increasing and CO was decreasing. In addition, faradic efficiency of ethylene on 10 bar is greater than 4 and 3 times at 3 and 5 bar, respectively. Meanwhile, the mass transfer of CO intermediate on the I-Cu foam can be accelerated to C-C coupling at higher pressure [2, 15, 23]. At 3 bar, faradic efficiency of CO and ethylene are lowest because CO intermediate are replaced by H intermediate on surface. So, Hydrogen evolution reaction are dominant than  $CO_2$  reduction at the cathode [1, 15]. The highest faradic efficiency of ethylene values of 33% at 5V and 10 bar.

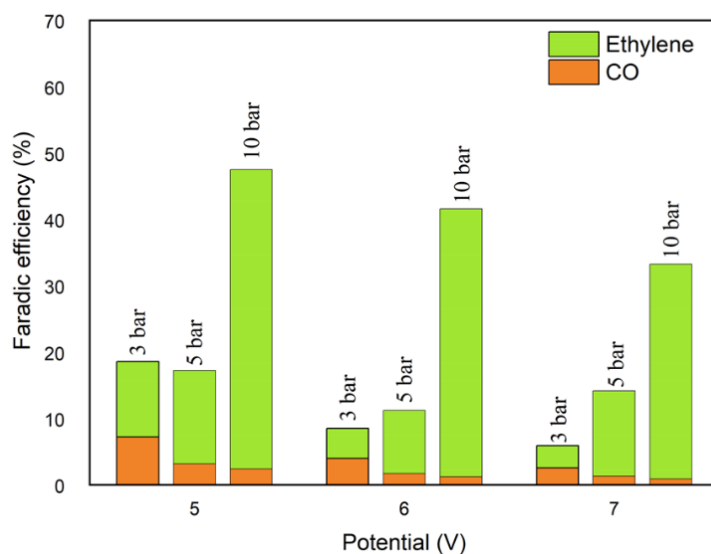


Figure 19 Effect of pressure on the electrochemical reduction of CO<sub>2</sub> on I-Cu foam.

#### 4.4 Effect of cell voltage

Fig.22 compares the faradic efficiency of CO and ethylene at 5, 6, and 7 V and 3, 5, and 10 bar, the result show at 5 V in each pressure were suggested that optimize applied voltage for electrochemical tubular reactor. In addition, low potential is selectively to formation of CO and ethylene. For increasing potential, total faradic efficiencies of both products were decreased that faradic efficiencies of CO were decrease and faradic efficiencies of ethylene were increased because CO intermediates are coupling to ethylene. Moreover, the current increased with cell voltage increased, total gas FE decreased with increasing voltage, corresponding to a shift toward liquid products at higher voltages[24].



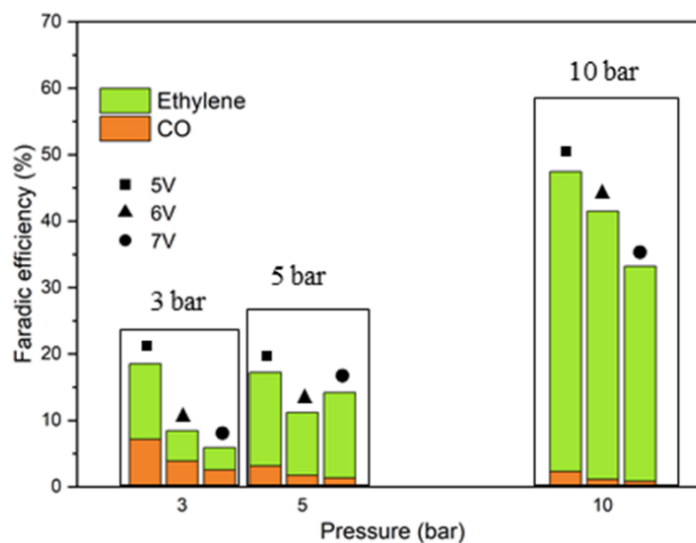


Figure 20 Effect of potential on the electrochemical reduction of CO<sub>2</sub> on I-Cu foam.

#### 4.5 Effect of type of gas

For observing the behavior of products from CO<sub>2</sub>ERR by using CO<sub>2</sub>, N<sub>2</sub>, and air feed for reactant gas and using I-Cu foam as a cathode at condition 3 bar with a CO<sub>2</sub> flow rate of 60 ml min<sup>-1</sup> and a trickling rate of CO<sub>2</sub>-saturated water of 1 ml min<sup>-1</sup> are shown in fig 25, The concentration of carbon monoxide and ethylene aren't produced when N<sub>2</sub> and air feed to CO<sub>2</sub>ERR in the electrochemical tubular fixed-bed reactor. In addition, N<sub>2</sub> feed as reactant gas was observed the behavior of CO and ethylene concentration wasn't occurred by using the inert gas. Meanwhile, CO concentration at condition CO<sub>2</sub> feed as reactant only occurred at the cathode. Moreover, single-chamber tubular fixed-bed electrochemical reactor for CO<sub>2</sub>ERR are design and study the effect of pressure but there are main problem that products from cathode and anode (e.g. CO<sub>2</sub>, CO, C<sub>2</sub>H<sub>4</sub>, and O<sub>2</sub>) are mixed in the single-chamber but we also confirmed the O<sub>2</sub> concentration weren't reduced at cathode by air feed condition as shown in fig.25. Moreover, air feed can prove the hypothesize for electrochemical can be in series in the future. Furthermore, this system uses water as a reactant in an electrochemical tubular reactor. To provide comparison, a

conventional electrochemical reduction reactor that utilized salt solution (e.g.  $\text{NaHCO}_3$  and  $\text{KHCO}_3$ ) as the reactant. Salt can act as a corrosion agent in the reactor.

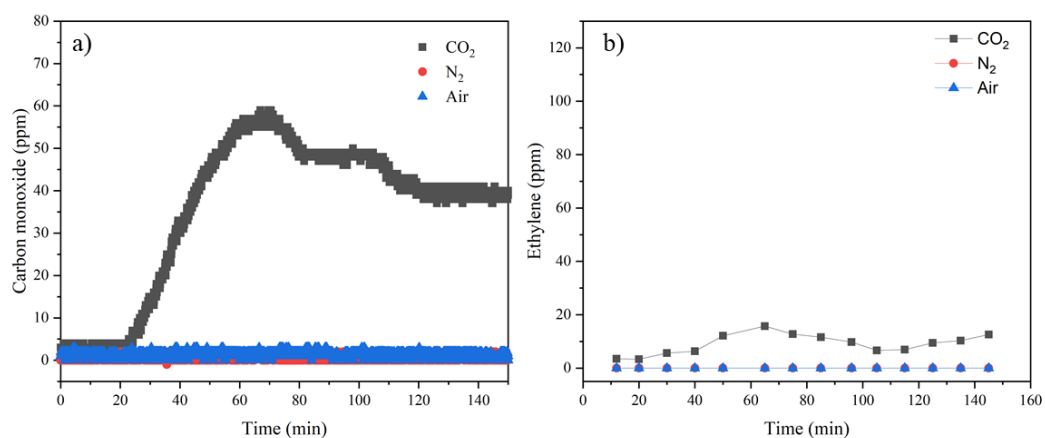
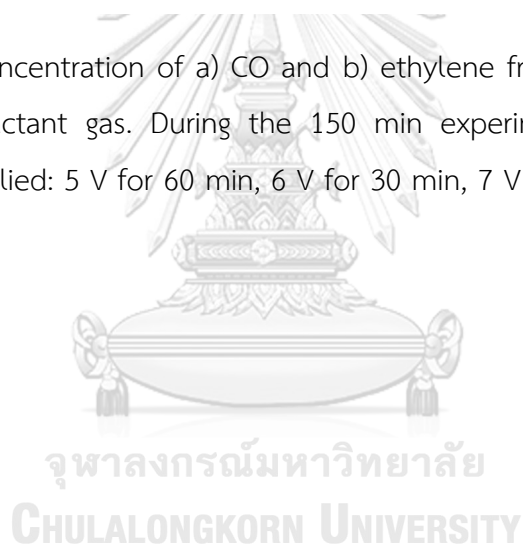


Figure 21 The concentration of a) CO and b) ethylene from I-Cu foam at different  $60 \text{ ml min}^{-1}$  reactant gas. During the 150 min experiments, the following cell voltages were applied: 5 V for 60 min, 6 V for 30 min, 7 V for 30 min and 8 V for 30 min.



## CHAPTER 5

### CONCLUSIONS and SUGGESTIONS

#### 5.1 Conclusions

The performance of CO<sub>2</sub>ERR is observed by the behavior of carbon monoxide and ethylene production with a CO<sub>2</sub> flow rate of 60 ml min<sup>-1</sup> and a trickling rate of CO<sub>2</sub>-saturated water of 1 ml min<sup>-1</sup>. During the 10 min experiments, the following cell voltages were applied: 5 V for 60 min, 6 V for 30 min, and 7 V for 30 min. The ionomer effect on copper foam represents the faradic efficiencies of CO and ethylene from I-Cu foam is greater than Cu foam at condition 3 bar in each cell voltage, so ionomer can improve the performance of CO<sub>2</sub>ERR on surface of copper foam and change pathway for CO<sub>2</sub> reduction.

Considering the effect of CO<sub>2</sub> pressure and potential, During the 150 min experiments, the following cell voltages were applied: 5 V for 60 min, 6 V for 30 min, and 7 V for 30 min. that ethylene concentration are increased and CO concentration are decreased when pressure increased. the ethylene and CO concentration are otherwise trended because CO intermediate more adsorb on I-Cu foam's surface and suppress H intermediate adsorption. So, CO<sub>2</sub> reduction can produce more carbon products, be accelerated to C-C coupling and inhibit H<sub>2</sub> evolution reaction.

The performance of CO<sub>2</sub>ERR is confirmed by N<sub>2</sub> feed for reactant. The CO and ethylene concentration using I-Cu foam as cathode doesn't occur in this system. In addition, the concentration of CO and ethylene only occurs at the cathode. Moreover, the electrochemical tubular fixed bed reactor is easy to operate and clean system. Also, it doesn't produce corrosive salt.

## 5.2 Suggestions

By-products including  $H_2$  and  $O_2$  from  $CO_2$  reduction in the electrochemical should detect and analyze to study the behavior.

The thickness of resin should be optimized for decreased resistance between  $CO_2$ ERR cell.





## APPENDIX A

### FARADIC EFFICIENCY CALCULATION

#### A.1 Faradic efficiency

Faradic efficiency of electrochemical CO<sub>2</sub>ERR is calculated by number of moles of electrons for producing product ( $e_{\text{output}}$ ) divided by total number of mole of electrons transferred in cell ( $e_{\text{input}}$ ) as follow

$$FE(\%) = \frac{e_{\text{output}}}{e_{\text{input}}} \times 100$$

Number of moles of electrons for producing product ( $e_{\text{output}}$ ):

$$e_{\text{output}} = y \int n \, dt$$

Where,

$y$  is a number of electrons required to produced product from half-cell reaction of C<sub>2</sub>H<sub>4</sub>.

$n$  is an amount of product (mol)

Total number of moles of electrons transferred in cell ( $e_{\text{input}}$ )

$$e_{\text{input}} = \frac{Q}{F}; Q = \int I \, dt$$

Where,

$I$  is a recorded current (A)

$t$  is required time (sec)

$F$  is Faraday constant (96485 C mol<sub>e</sub><sup>-1</sup>)

Table 4 Data of ethylene concentration from GC. ( $\text{CO}_2$  60 ml  $\text{min}^{-1}$  and  $\text{H}_2\text{O}$  1 ml  $\text{min}^{-1}$ )

Cathode	Pressure (bar)	$\int n dt$ (ppm min)		
		Potential (V)		
		5	6	7
Cu foam	3	83.1	141.937	74.187
I-Cu foam	3	281.719	188.909	179.606
I-Cu foam	5	657.18	679.857	993.005
I-Cu foam	10	1205.889	1808.06	1903.817

Table 5 Data of CO concentration from IR. ( $\text{CO}_2$  60 ml  $\text{min}^{-1}$  and  $\text{H}_2\text{O}$  1 ml  $\text{min}^{-1}$ )

Cathode	Pressure (bar)	$\int n dt$ (ppm min)		
		Potential (V)		
		5	6	7
Cu foam	3	892.783	968.75	883.475
I-Cu foam	3	1067.4	966.091	798.65
I-Cu foam	5	885.458	737.483	601.3
I-Cu foam	10	369.85	306.017	294.592

Table 6 Data of current from potentialstat . (CO<sub>2</sub> 60 ml min<sup>-1</sup> and H<sub>2</sub>O 1 ml min<sup>-1</sup>)

Cathode	Pressure (bar)	$\int I dt$ (mA min)		
		Potential (V)		
		5	6	7
Cu foam	3	112.543	213.768	225.874
I-Cu foam	3	117.541	195.746	252.233
I-Cu foam	5	220.997	338.781	364.992
I-Cu foam	10	126.461	212.033	278.594

Example for faradic efficiency of C<sub>2</sub>H<sub>4</sub> calculation for Cu foam at 5V and 3 bar.

$$e_{\text{output}} = y \int n dt$$

When,

$$y = 12 \text{ from eq.8}$$

$$\int n dt = \int \text{ppm}_{\text{C}_2\text{H}_4} dt \times \frac{60 \text{ ml}}{\text{min}} \times \frac{\text{K mol}}{8.314 \text{ m}^3 \text{ Pa}} \times \frac{101325 \text{ Pa}}{\text{atm}} \times \frac{1}{298.15 \text{ K}} \times \frac{1}{10^6} \times \frac{\text{m}^3}{10^6 \text{ ml}}$$

$$\int n dt = 2.038 \times 10^{-7} \text{ mol}_{\text{C}_2\text{H}_4}$$

So,

$$e_{\text{output}} = \frac{12 \text{ mol } e^-}{1 \text{ mol } \text{C}_2\text{H}_4} \times 2.038 \times 10^{-7} \text{ mol}_{\text{C}_2\text{H}_4}$$

$$e_{\text{output}} = 2.446 \times 10^{-6} \text{ mol } e^-$$



$$e_{\text{input}} = \frac{Q}{F}; Q = \int I dt$$

When,

$$e_{\text{input}} = \frac{\int I dt}{F}$$

$$e_{\text{input}} = 112.543 \text{ mA min} \times \frac{\text{mol } e^-}{96485 \text{ A s}} \times \frac{\text{A}}{1000 \text{ mA}} \times \frac{60 \text{ s}}{\text{min}}$$

$$e_{\text{input}} = 6.999 \times 10^{-5} \text{ mol } e^-$$

$$\text{FE}(\%) = \frac{e_{\text{output}}}{e_{\text{input}}} \times 100$$

$$\text{FE}(\%) = \frac{2.446 \times 10^{-6} \text{ mol } e^-}{6.99 \times 10^{-5} \text{ mol } e^-} \times 100$$

$$\text{FE}(\%) = 3.50$$

## APPENDIX B

## CHARACTERIZATION of CATHODES

## B.1 XRD

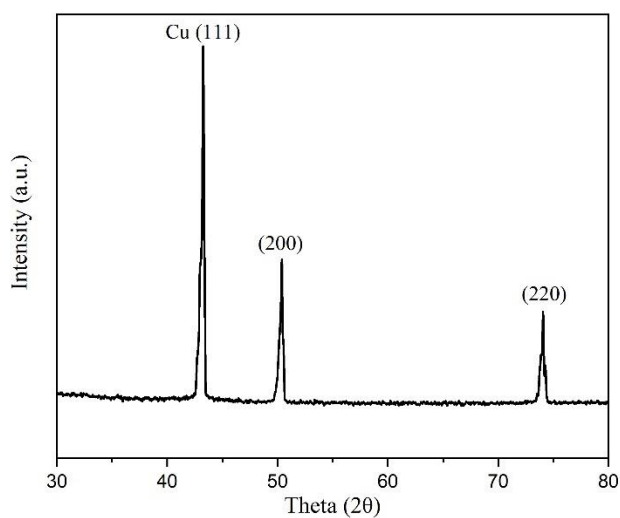


Figure 22 XRD of copper powder

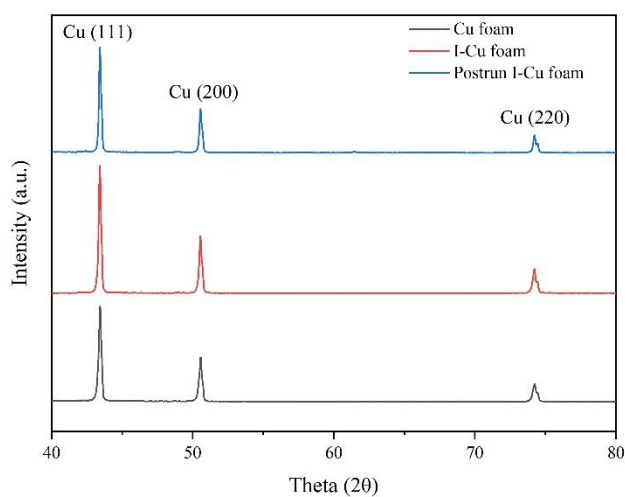


Figure 23 XRD of fresh Cu foam, I-Cu foam and post run I-Cu foam.

## B.2 SEM

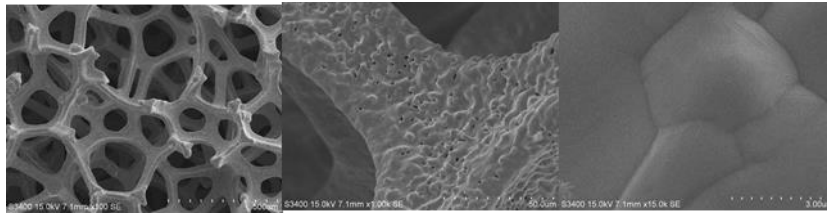


Figure 24 SEM of fresh Cu foam.

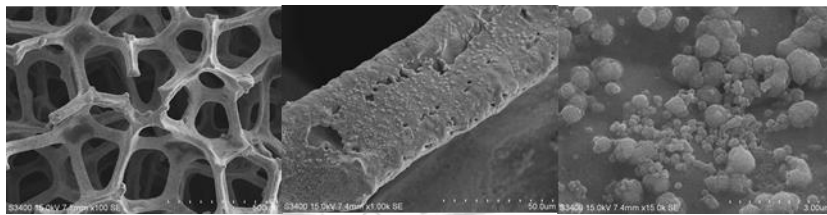


Figure 25 SEM of fresh I-Cu foam.



Figure 26 SEM of fresh Cu-elec.

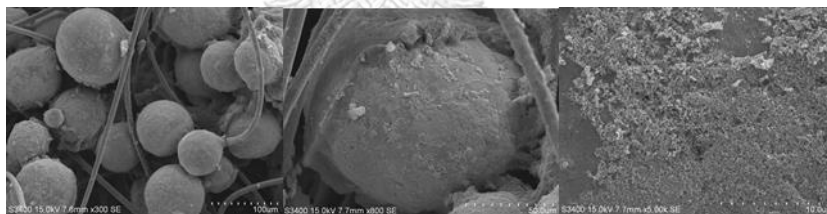


Figure 27 SEM of fresh Cu-ink.

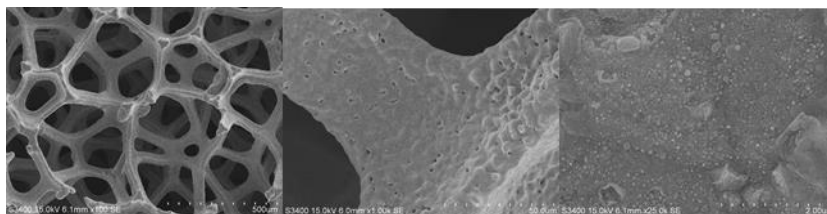


Figure 28 SEM of post run Cu foam at 3 bar.

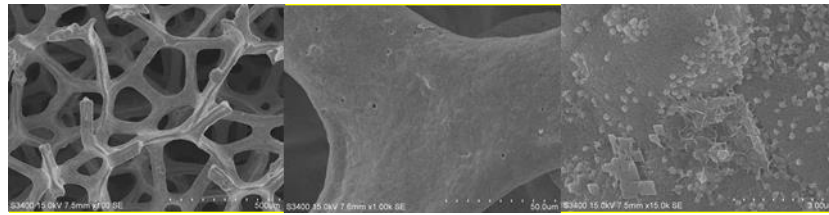


Figure 29 SEM of post run I-Cu foam at condition 3 bar.

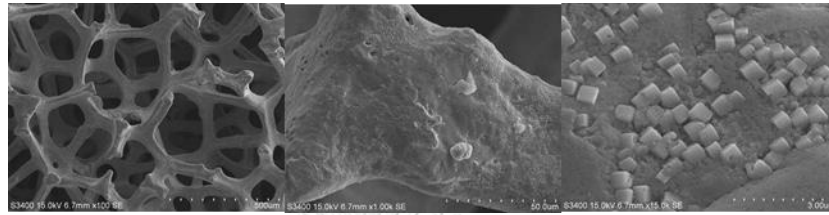


Figure 30 SEM of post run I-Cu foam at condition 5 bar.

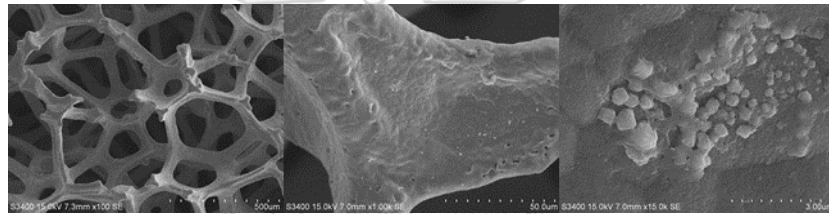


Figure 31 SEM of post run I-Cu foam at condition 10 bar.

### B.3 EDX

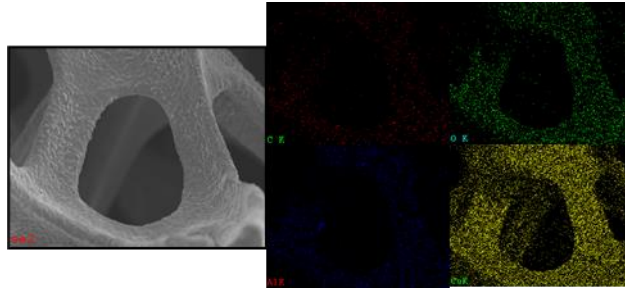


Figure 32 element dispersion of fresh Cu foam.

Table 7 element dispersion of fresh Cu foam.

Element	Wt%	At%
CK	00.91	04.39
OK	02.05	07.38
ALK	00.19	00.41
CuK	96.84	87.82
Matrix	100	100

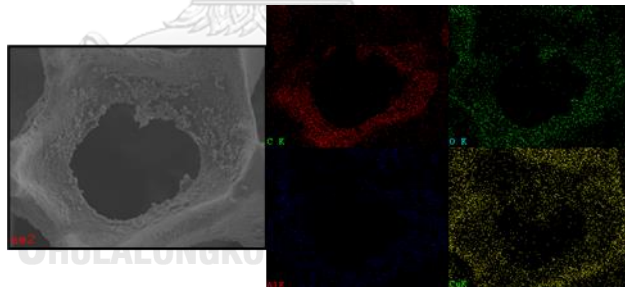


Figure 33 SEM of fresh I-Cu foam.

Table 8 element dispersion of I-Cu foam.

Element	Wt%	At%
CK	22.80	55.60
OK	06.35	11.63
ALK	00.17	00.19
CuK	70.67	32.58
Matrix	100	100

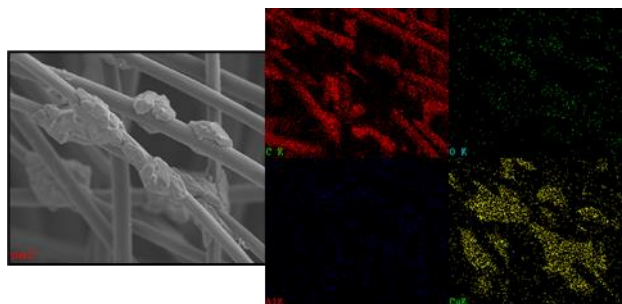


Figure 34 SEM of fresh Cu-elec.

Table 9 element dispersion of Cu-elec.

Element	Wt%	At%
CK	52.20	84.40
OK	01.03	01.25
ALK	00.15	00.11
CuK	46.62	14.25
Matrix	100	100

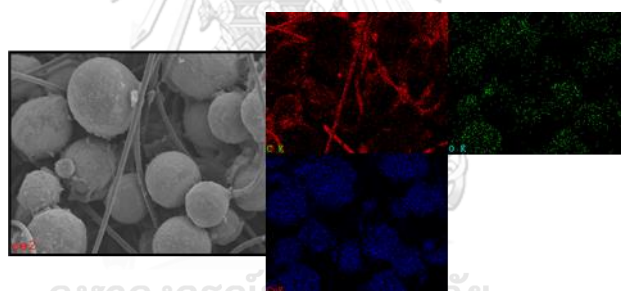


Figure 35 SEM of fresh Cu-ink.

Table 10 element dispersion of Cu-ink.

Element	Wt%	At%
CK	35.98	73.29
OK	01.80	02.76
CuK	62.22	23.96
Matrix	100	100

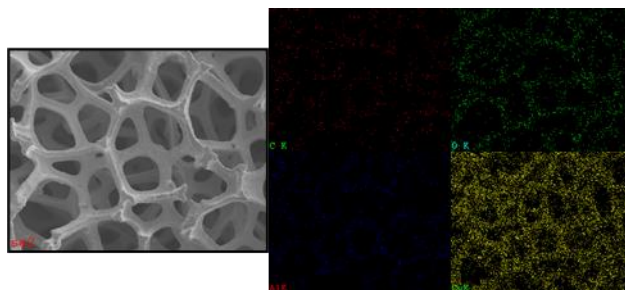


Figure 36 SEM of post run Cu foam at condition 3 bar.

Table 11 element dispersion of post run Cu foam at condition 3 bar.

Element	Wt%	At%
CK	01.51	07.11
OK	02.04	07.19
ALK	00.14	00.29
CuK	96.30	85.41
Matrix	100	100

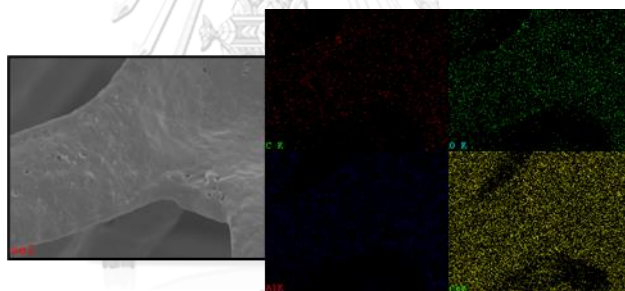


Figure 37 SEM of post run I-Cu foam at condition 3 bar.

Table 12 element dispersion of post run I-Cu foam at condition 3 bar.

Element	Wt%	At%
CK	00.93	04.47
OK	02.03	07.30
ALK	00.20	00.43
CuK	96.84	87.80
Matrix	100	100

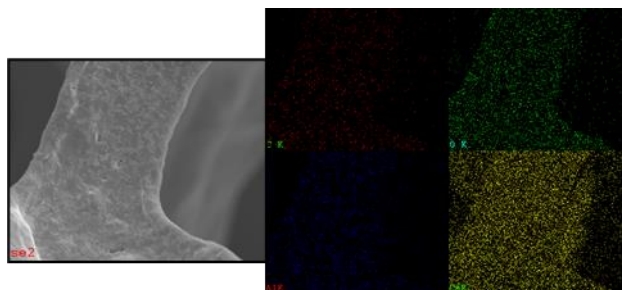


Figure 38 SEM of post run I-Cu foam at condition 5 bar.

Table 13 element dispersion of post run I-Cu foam at condition 5 bar.

Element	Wt%	At%
CK	02.61	10.81
OK	04.27	13.29
ALK	02.74	05.05
CuK	90.39	70.85
Matrix	100	100

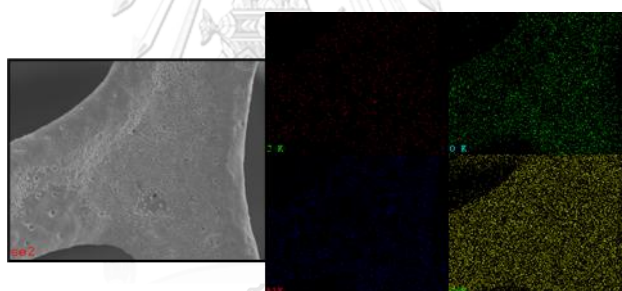


Figure 39 SEM of post run I-Cu foam at condition 10 bar.

Table 14 Element dispersion of post run I-Cu foam at condition 10 bar.

Element	Wt%	At%
CK	01.19	05.40
OK	03.95	13.41
ALK	00.13	00.26
CuK	94.72	80.93
Matrix	100	100



## APPENDIX C

## ELECTROCHEMICAL REDUCTION PERFORMANCE

C.1 Faradic efficiency of products in each condition.

Table 15 Faradic efficiency of CO and ethylene for 20 min. ( $\text{H}_2\text{O}$  1 ml min<sup>-1</sup> and  $\text{CO}_2$  60 ml min<sup>-1</sup>)

Cathode	Pressure (bar)	Faradic efficiency (%)					
		Potential (V)					
		5		6		7	
		CO	C <sub>2</sub> H <sub>4</sub>	CO	C <sub>2</sub> H <sub>4</sub>	CO	C <sub>2</sub> H <sub>4</sub>
Cu foam	3	6.25	3.50	3.57	3.14	3.08	1.55
I-Cu foam	3	7.16	11.34	3.89	4.56	2.49	3.37
I-Cu foam	5	3.16	14.07	1.71	9.49	1.29	12.87
I-Cu foam	10	2.30	45.13	1.13	40.35	0.83	32.34

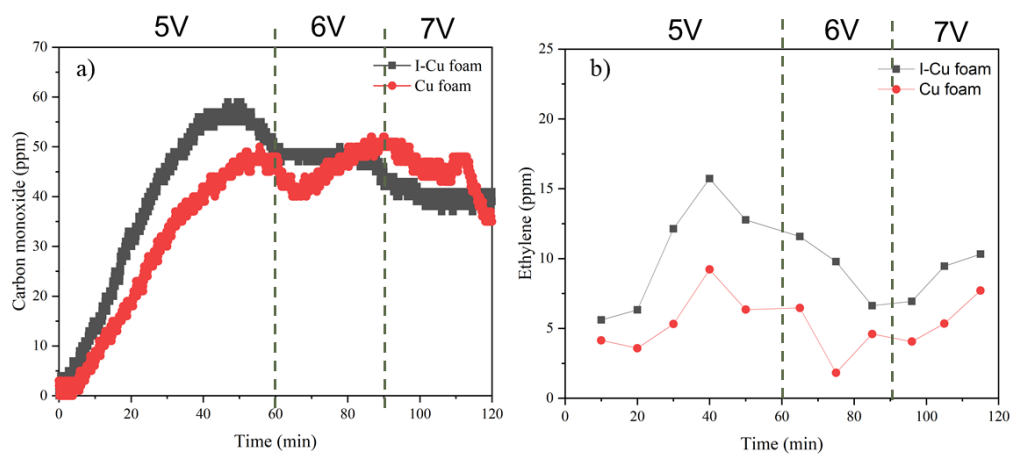


Figure 40 The concentration of a) CO and b) ethylene from Cu foam and I-Cu foam at 3 bar. During the 120 min experiments, the following cell voltages were applied: 5 V for 60 min, 6 V for 30 min and 7 V for 30 min.

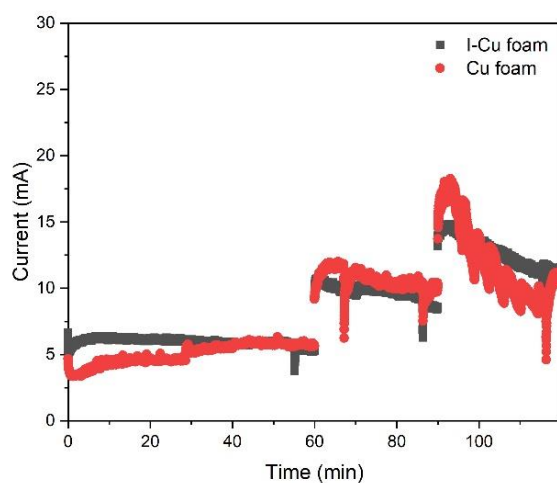


Figure 41 The current density for Cu foam and I-Cu foam at condition 3 bar. During the 120 min experiments, the following cell voltages were applied: 5 V for 60 min, 6 V for 30 min, and 7 V for 30 min.

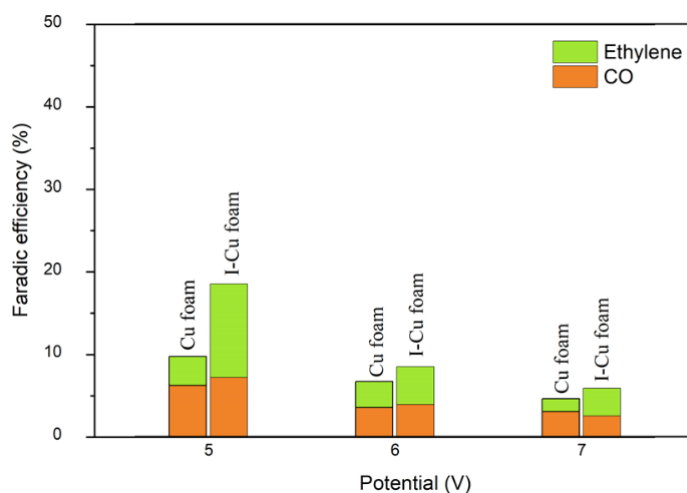


Figure 42 Effect of ionomer (sustainion XA9) on the electrochemical reduction of  $\text{CO}_2$  on Cu foam and I-Cu foam at 3 bar.

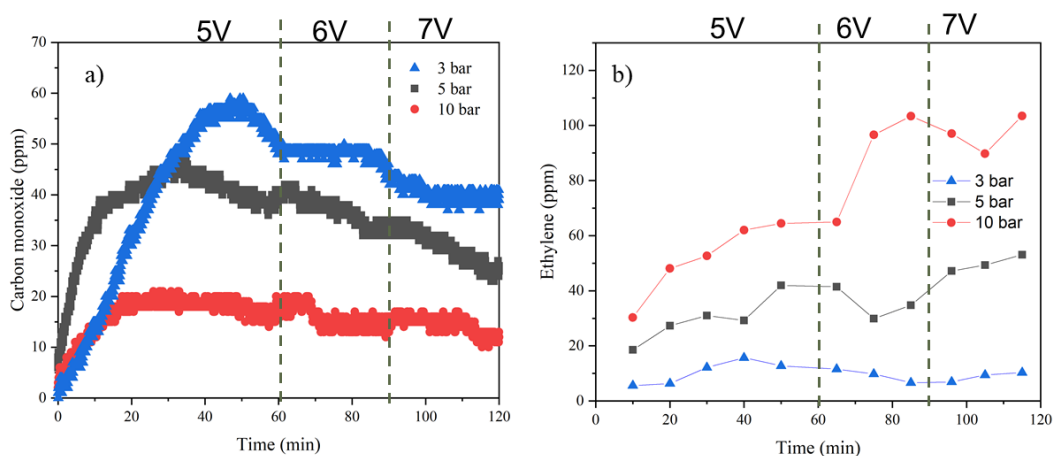


Figure 43 The concentration of a) CO and b) ethylene from I-Cu foam at different pressure. During the 150 min experiments, the following cell voltages were applied: 5 V for 60 min, 6 V for 30 min and 7 V for 30 min.

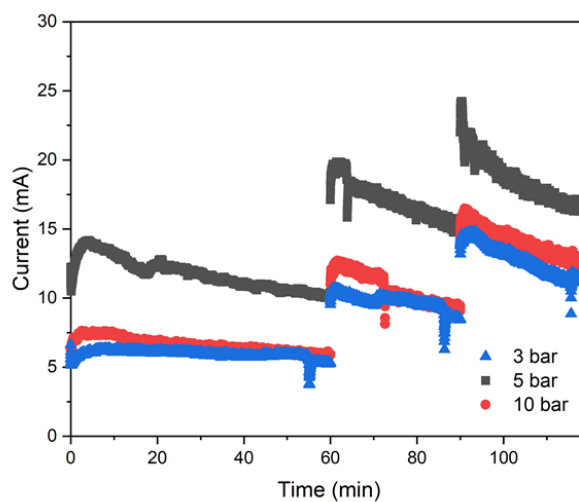


Figure 44 The current for I-Cu foam at different pressure. During the 150 min experiments, the following cell voltages were applied: 5 V for 60 min, 6 V for 30 min, and 7 V for 30 min.

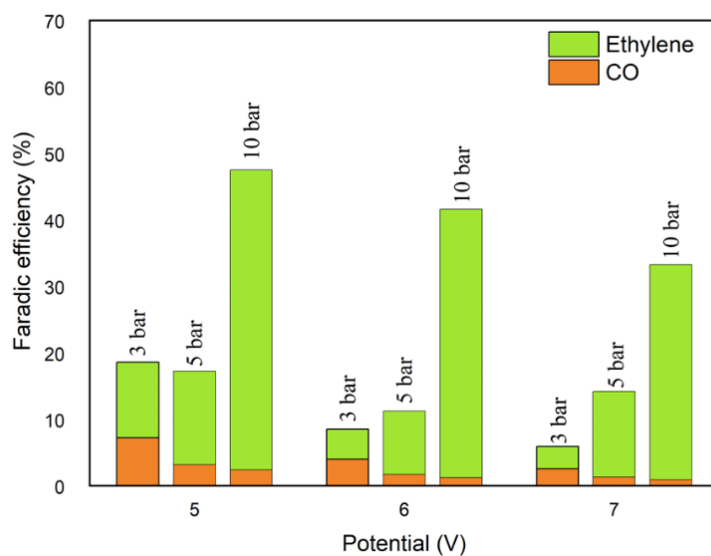


Figure 45 Effect of pressure on the electrochemical reduction of  $\text{CO}_2$  on I-Cu foam.

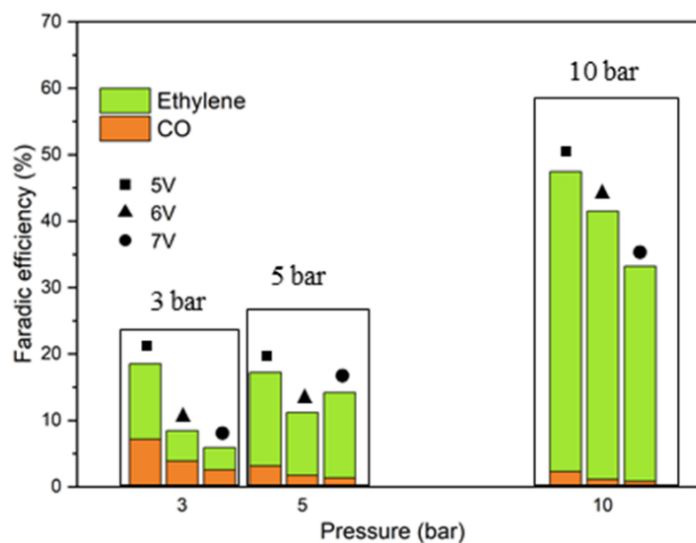


Figure 46 Effect of potential on the electrochemical reduction of CO<sub>2</sub> on I-Cu foam.

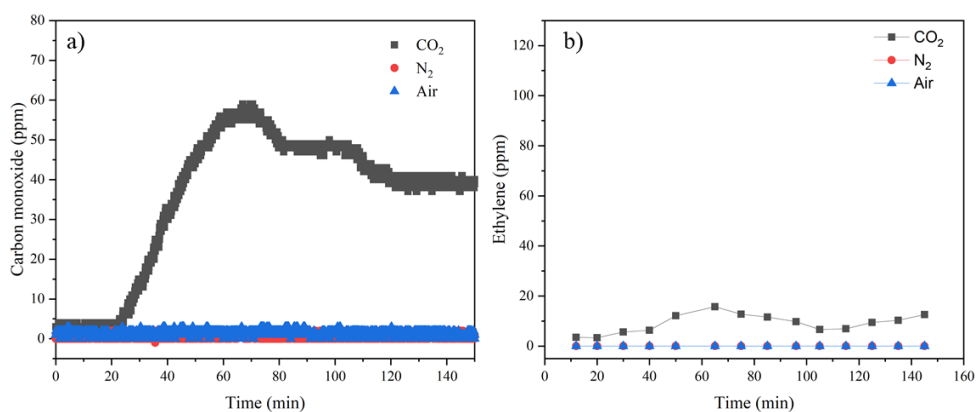


Figure 47 The concentration of a) CO and b) ethylene from I-Cu foam at different 60 ml min<sup>-1</sup> reactant gas. During the 150 min experiments, the following cell voltages were applied: 5 V for 60 min, 6 V for 30 min, 7 V for 30 min and 8 V for 30 min.

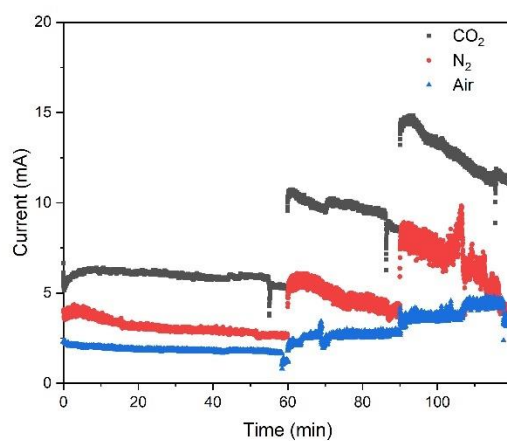
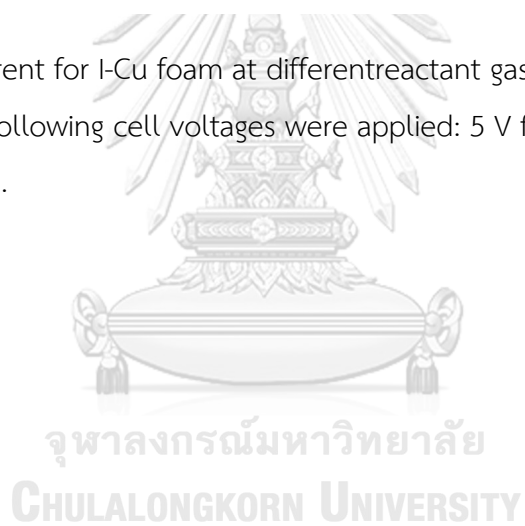


Figure 48 The current for I-Cu foam at different reactant gas. During the 150 min experiments, the following cell voltages were applied: 5 V for 60 min, 6 V for 30 min, and 7 V for 30 min.



## REFERENCES

1. Ye W, Guo X, Ma T. A review on electrochemical synthesized copper-based catalysts for electrochemical reduction of CO<sub>2</sub> to C<sub>2+</sub> products. *Chemical Engineering Journal*. 2021;414.
2. Kas R, Kortlever R, Yilmaz H, Koper MTM, Mul G. Manipulating the Hydrocarbon Selectivity of Copper Nanoparticles in CO<sub>2</sub> Electroreduction by Process Conditions. *ChemElectroChem*. 2015;2(3):354-8.
3. Gao Y, Wu Q, Liang X, Wang Z, Zheng Z, Wang P, et al. Cu<sub>2</sub>O Nanoparticles with Both {100} and {111} Facets for Enhancing the Selectivity and Activity of CO<sub>2</sub> Electroreduction to Ethylene. *Adv Sci (Weinh)*. 2020;7(6):1902820.
4. Kortlever R, Shen J, Schouten KJ, Calle-Vallejo F, Koper MT. Catalysts and Reaction Pathways for the Electrochemical Reduction of Carbon Dioxide. *J Phys Chem Lett*. 2015;6(20):4073-82.
5. Sun Z, Ma T, Tao H, Fan Q, Han B. Fundamentals and Challenges of Electrochemical CO<sub>2</sub> Reduction Using Two-Dimensional Materials. *Chem*. 2017;3(4):560-87.
6. Nitopi S, Bertheussen E, Scott SB, Liu X, Engstfeld AK, Horch S, et al. Progress and Perspectives of Electrochemical CO<sub>2</sub> Reduction on Copper in Aqueous Electrolyte. *Chem Rev*. 2019;119(12):7610-72.
7. Ni Z, Liang H, Yi Z, Guo R, Liu C, Liu Y, et al. Research progress of electrochemical CO<sub>2</sub> reduction for copper-based catalysts to multicarbon products. *Coordination Chemistry Reviews*. 2021;441.
8. Kuo L, Dinh C-T. Toward efficient catalysts for electrochemical CO<sub>2</sub> conversion to C<sub>2</sub> products. *Current Opinion in Electrochemistry*. 2021;30.
9. Liu A, Gao M, Ren X, Meng F, Yang Y, Gao L, et al. Current progress in electrocatalytic carbon dioxide reduction to fuels on heterogeneous catalysts. *Journal of Materials Chemistry A*. 2020;8(7):3541-62.
10. Raciti D, Wang C. Recent Advances in CO<sub>2</sub> Reduction Electrocatalysis on Copper. *ACS Energy Letters*. 2018;3(7):1545-56.

11. Besra L, Liu M. A Review on Fundamentals and Applications of Electrophoretic Deposition (EPD). *Progress in Materials Science*. 2007;52:1-61.
12. Hori Y, Wakebe H, Tsukamoto T, Koga O. Adsorption of CO accompanied with simultaneous charge transfer on copper single crystal electrodes related with electrochemical reduction of CO<sub>2</sub> to hydrocarbons. *Surface Science*. 1995;335:258-63.
13. Hori Y, Takahashi I, Koga O, Hoshi N. Selective Formation of C<sub>2</sub> Compounds from Electrochemical Reduction of CO<sub>2</sub> at a Series of Copper Single Crystal Electrodes. *The Journal of Physical Chemistry B*. 2002;106(1):15-7.
14. Zhang B, Zhang J, Hua M, Wan Q, Su Z, Tan X, et al. Highly Electrocatalytic Ethylene Production from CO<sub>2</sub> on Nanodeficient Cu Nanosheets. *J Am Chem Soc*. 2020;142(31):13606-13.
15. Hara K, Tsuneto A, Kudo A, Sakata T. Electrochemical Reduction of CO<sub>2</sub> on a Cu Electrode under High Pressure: Factors that Determine the Product Selectivity. *Journal of The Electrochemical Society*. 1994;141(8):2097-103.
16. Hori Y, Murata A, Takahashi R, Suzuki S. Electroreduction of carbon monoxide to methane and ethylene at a copper electrode in aqueous solutions at ambient temperature and pressure. *Journal of the American Chemical Society*. 1987;109(16):5022-3.
17. Popović S, Smiljanić M, Jovanović P, Vavra J, Buonsanti R, Hodnik N. Stability and degradation mechanisms of copper-based catalysts for electrochemical CO<sub>2</sub> reduction. *Angewandte Chemie*. 2020;132(35):14844-54.
18. Wang H, Wang R, Sui S, Sun T, Yan Y, Du S. Cathode design for proton exchange membrane fuel cells in automotive applications. *Automotive Innovation*. 2021;4(2):144-64.
19. Liu Z, Yang H, Kutz R, Masel RI. CO<sub>2</sub> electrolysis to CO and O<sub>2</sub> at high selectivity, stability and efficiency using sustainion membranes. *Journal of The Electrochemical Society*. 2018;165(15):J3371.
20. Hori Y, Murata A, Yoshinami Y. Adsorption of CO, intermediately formed in electrochemical reduction of CO<sub>2</sub>, at a copper electrode. *Journal of the Chemical Society, Faraday Transactions*. 1991;87(1):125-8.



21. Kim JJ, Summers DP, Frese KW. Reduction of CO<sub>2</sub> and CO to methane on Cu foil electrodes. *Journal of Electroanalytical Chemistry and Interfacial Electrochemistry*. 1988;245(1):223-44.
22. Hara K, Tsuneto A, Kudo A, Sakata T. Electrochemical reduction of CO<sub>2</sub> on a Cu electrode under high pressure: factors that determine the product selectivity. *Journal of the Electrochemical Society*. 1994;141(8):2097.
23. Song H, Song JT, Kim B, Tan YC, Oh J. Activation of C<sub>2</sub>H<sub>4</sub> reaction pathways in electrochemical CO<sub>2</sub> reduction under low CO<sub>2</sub> partial pressure. *Applied Catalysis B: Environmental*. 2020;272:119049.
24. Gabardo CM, Seifitokaldani A, Edwards JP, Dinh C-T, Burdyny T, Kibria MG, et al. Combined high alkalinity and pressurization enable efficient CO<sub>2</sub> electroreduction to CO. *Energy & Environmental Science*. 2018;11(9):2531-9.





จุฬาลงกรณ์มหาวิทยาลัย  
**CHULALONGKORN UNIVERSITY**

## VITA

**NAME** Kanjira Janya

**DATE OF BIRTH** 3 Sep 1997

**PLACE OF BIRTH** Chanthaburi

**INSTITUTIONS ATTENDED** Mahidol University, 2016-2010  
Bachelor of Engineering (B.Eng)

**HOME ADDRESS** 56 Saikhao Soidao Chanthaburi,Thailand 22180

**AWARD RECEIVED** Best poster presentation for "Production of Ethylene in Electrochemical Reduction of Carbon Dioxide at Copper Electrode in the Novel Electrochemical Tubular Fixed Bed Reactor" in Pure and Applied Chemistry International Conference 2022